1960

High temperature oxidation of nickel

Virgil R. Friebel

Department:

HIGH TEMPERATURE OXIDATION OF NICKEL

BY

Virgil R. Friebel

A

THESIS

submitted to the faculty of the

SCHOOL OF MINES AND METALLURGY OF THE UNIVERSITY OF MISSOURI

in partial fulfillment of the work required for the

Degree of

MASTER OF SCIENCE IN METALLURGICAL ENGINEERING

Rolla, Missouri

1960

Approved by

Andrew Larson (Advisor)

J. E. Thomason

W. T. Schrenk

ABSTRACT

Using a sensitive volumetric technique, a study was made of the kinetics of oxidation of nickel at 1200° C. and 1300° C. Three purities of nickel were used for the investigation which was limited to the initial three hours of reaction.

The rate of oxidation of nickel followed the parabolic rate law after an initial period of deviation which lasted up to 40 minutes. No direct correlation was found between the oxide thickness and the end of the period of deviation from the parabolic rate law.

The purity of the nickel was found to have a marked effect on the rate of oxidation of nickel which increased as the purity decreased.

The color of the oxide on nickel was found to be related to the thickness of the oxide layer. The oxide on high-purity nickel was gray initially but rapidly changed to green and then gradually to black with thickening.

PREFACE

The writer wishes to express his appreciation to Mr. J. A. Rowland (Director of the Rolla Metallurgy Research Center) and others who made it possible for this investigation to be conducted under a Fellowship from the U. S. Bureau of Mines. The Bureau of Mines furnished the space and equipment and valuable assistance needed for the completion of this investigation.

The writer wishes to thank Dr. A. H. Larson, who was the faculty advisor for this research project, and R. M. Doerr, whose guidance and assistance aided considerably in the completion of the project. The valuable informal discussions with various faculty members and Bureau of Mines employees and the excellent cooperation and assistance received from Bureau of Mines employees is gratefully acknowledged.

The excellent high-purity nickel was furnished by the International Nickel Company.

TABLE OF CONTENTS

LIST OF FIGURES

LIST OF TABLES

I. INTRODUCTION

This investigation is the result of the interest of the U. S. Bureau of Mines and the author in high temperature oxidation of metals and alloys. The volumetric technique was used to measure the rate of oxidation at the request of the U. S. Bureau of Mines. The Bureau of Mines had a gravimetric apparatus in operation and desired a sensitive method which could continue to function even if spallation of the oxide occurred.

The interest in high temperature oxidation of metals has developed along with the development of new uses for metals and alloys at elevated temperatures. The possibility of using a metal or alloy at high temperatures often depends on the degree of protection from further oxidation offered by the oxide film. The protection against oxidation usually increases as the thickness of the oxide film increases. At some limiting temperature, the rate of oxidation may increase and no longer depend on the thickness of the oxide film. Loss of protection may be due to volatilization of the metal or the oxide, melting of the oxide, or loss of adhesion of the oxide to the metal.

Gulbransen and Andrew reported that at 1000° C. and higher the oxide cracks away from nickel and protection fails to increase with thickening of the oxide.[1] Doerr, of the U. S. Bureau of Mines, found in preliminary tests with low purity nickel that the oxide offered increased protection with thickening at 1200° C.[2]

The purpose of this investigation was to construct a volumetric apparatus for measuring the rate of oxidation and to apply this apparatus to the oxidation of nickel at elevated temperatures. The apparatus used was a modification of an apparatus developed by Jenkins.[3]

Initial tests were made with low-purity nickel prior to the arrival of high-purity (99.99+%) nickel. The rate of oxidation was measured at 1200° C. and 1300° C. A microscopic examination was made on the oxide film and as a check for internal oxidation.

II. REVIEW OF LITERATURE

Previous Research. The rate of oxidation of nickel has been studied in several investigations in the past. A search of the literature was made and only one specific reference was found concerning the oxidation of nickel at 1200° C. Frederick and Cornet investigated the rate of oxidation of nickel and nickel-cobalt alloys up to 1400° C.[4] Due to malfunctioning of the equipment, these investigators were unable to measure the rate of oxidation accurately and assumed that the parabolic rate law applied for calculations based on total weight change. They also overlooked the possible effect of moisture and made no attempt to dry the air in the oxidation zone.

Preece and Lucas oxidized nickel at temperatures up to 1075° C.[5] A plot was made of the weight gained per unit area after 24 hours. Their results gave a smooth curve which indicated no radical change in the oxidation process up to 1075° C. They found that nickel oxidized preferentially at the grain boundaries. These investigators also reported that the oxide layer on nickel was comprised of two layers; a dark-green coherent outer layer and a light-green powdery inner layer. Both layers were reported to be NiO.

Uhlig, Pickett, and MacNairn reported that the oxidation rate of nickel followed the logarithmic law in the temperature range 300° - 450° C.[6] Moore and Lee reported that the rate of oxidation of nickel followed the parabolic rate law from 400° C. to 900° C.[7] Figure 1 shows the temperature effect for the range 750° - 1050° C. Figure 2 shows the effect of temperature for the range 400° - 750° C. Gulbransen and Andrew found that their data fit the parabolic rate law from 550° - 900° C. but over 900° C. the rate of oxidation of nickel

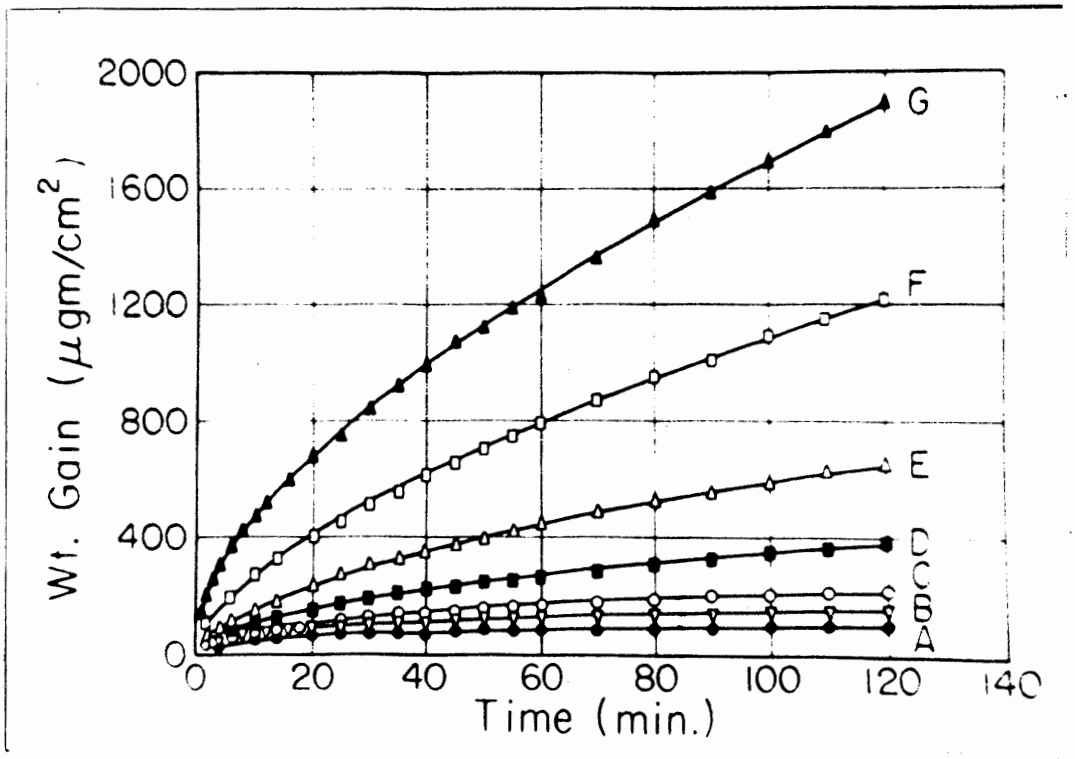

Figure 1. Effect of temperature on oxidation of nickel, 7.6 cm Hg of O_2. A, 750°C.; B, 800° C.; C, 850° C.; D, 900° C.; E, 950° C.; F, 1000° C.; G, 1050° C.[1]

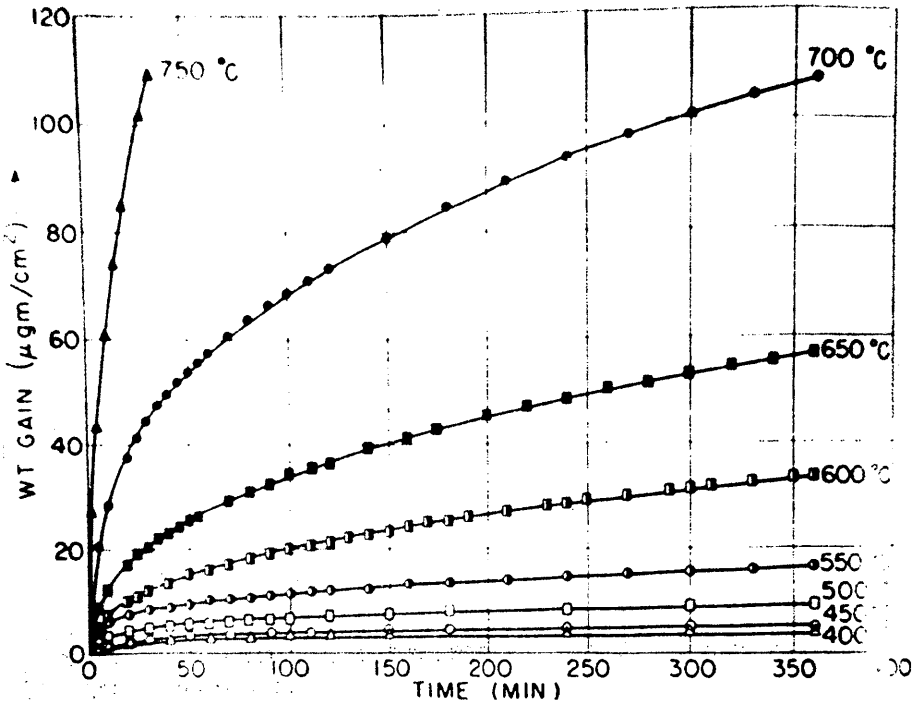

Figure 2. Effect of temperature, 400° - 750° C., on oxidation of nickel, 7.6 cm Hg of O_2.[8]

departed from the parabolic rate law.[1,8] They concluded that the failure was due to a localized loss of adhesion between the metal and the oxide. The basis for their conclusion was the change in color of the nickel oxide from gray to green at about 900° C. They claimed that the loss of adhesion between the metal and the oxide would interrupt the normal diffusion processes necessary for the oxidation to continue to follow the parabolic rate law. Cracking of the oxide may also accompany the loss of adhesion but no visible cracks were reported.

Gulbransen and Hickman carried out an electron diffraction study of oxide films formed on various metals at elevated temperatures.[9] They found that NiO was the only oxide that occurred on nickel in the range of 450° - 700° C.

Figure 3 shows the effect of purity on the oxidation rate constants of nickel. The nickel of lower purity was found to oxidize more rapidly by a factor of ten or more. The differences in results of many investigators can probably be partly attributed to different purities of nickel used for their experiments.

Methods of Investigation. A wide variety of methods have been used to measure the rate of oxidation of metals and alloys. The methods discussed here are those which have been most widely used in the past and have given comparable results.

The gravimetric method is the oldest and most popular method. This method measures the surface oxidation and also the internal or subsurface oxidation. It may be as simple as checking the weight gained by weighing before and after oxidation or as elaborate as a continuous-weighing microbalance with a recorder. Gulbransen developed a vacuum microbalance which has been the greatest single contribution to the gravimetric approach.[11]

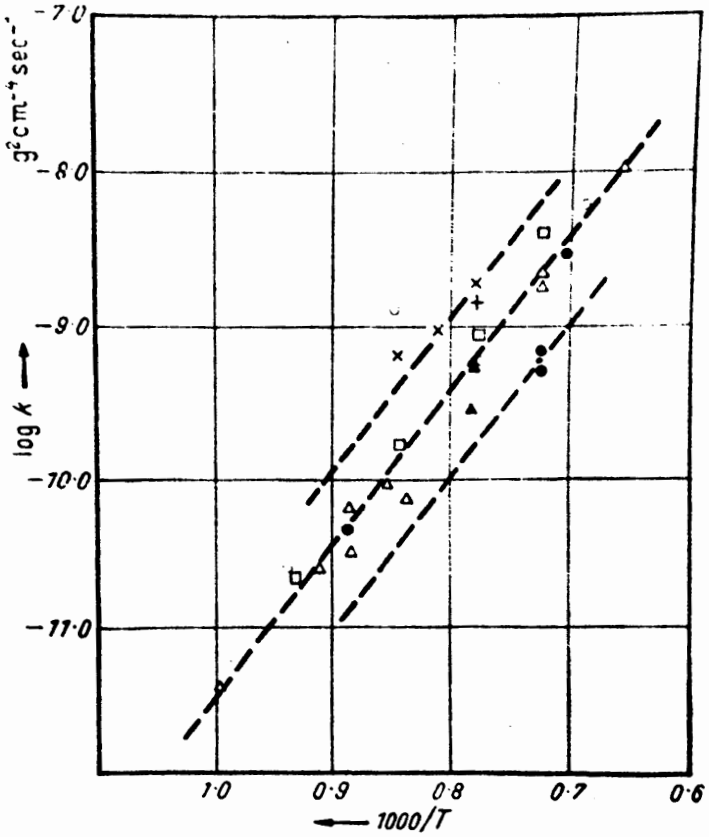

× Nickel 'A' (International Nickel Co.)
98·88% Ni
0·48% Fe
0·18% Mn
0·17% Si

+ Nickel (Heraeus Vakuumschmelze, Hanau)
0·5 to 1·0% Mn
some Fe
nil Mg

□ Electrolytic Nickel (International Nickel Co.)
99·67% Ni
0·25% Fe
0·03% C
0·04% Si
traces Mn

Δ 'Rein-Nickel'
0·07% Si
0·07% Cu
0·27% Fe
0·20% Co
0·01% Cr
0·01% Al
nil Mn

○ Carbonyl Nickel (I.G. Farbenindustrie)
0·04% C
0·12% Fe
0·09% O
nil S

▲ Electrolytic Ni remelted in vacuo

● Carbonyl Nickel remelted in vacuo

Figure 3. Effect of purity on the oxidation of nickel.[10]

Two other methods which have been used extensively are the manometric and volumetric methods. The manometric and volumetric methods are quite similar. They both depend on a gas-tight system and are complicated by thermal diffusion of the gases when a mixture of gases, such as air, is used. The gases with lower atomic weights tend to segregate in the zone of higher temperature and the heavier gases tend to concentrate in the coldest zone. Both methods can be very sensitive and allow continuous readings. Sample preparation is very important. Volatilization of surface contaminants or secondary gaseous reactions must be avoided. Campbell and Thomas have developed one of the most accurate manometric methods.[12] Jenkins has developed an excellent volumetric apparatus which was modified for this investigation.[3] Both methods measure internal or subsurface oxidation as well as surface oxidation.

There are several optical methods for measuring the rate of oxidation. The main one in use today is based on the use of polarized light. Tronstad developed an excellent process based on the fact that a change in the degree of polarization occurs when a beam of polarized light is reflected from a metal surface which is developing an oxide film.[13] Optical methods fail to measure internal oxidation and irregularities in the film surface may cause erroneous results.

The change in electrical resistance with oxidation has been used by many investigators. The change in resistance must be limited only to the decrease in cross-sectional area. Heat treatment during oxidation and preferential oxidation of alloys causes errors with the electrical resistance method.

Oxidation Rate Laws. The relationship between amount of oxidation and time is generally expressed by one of three rate laws. They are expressed here in terms of weight increase, W, and time, t.

Linear Rate Law . . . . . $W = K_1 t$

Parabolic Rate Law . . . . . $W^2 = K_2 t$

Logarithmic Rate Law . . . . . $W = K_3 \log (at+b)$

These empirical laws have very specialized applications. A metal may follow one law under one set of conditions and a different law under different conditions. The parabolic rate law is the only one which has been satisfactorily derived from theoretical considerations.

The linear rate law is applicable when the oxidation product offers no interference to contact between the metal surface and the gas phase. The metals and alloys which obey the linear rate law form either a volatile or a porous oxide.

The parabolic rate law was derived by Pilling and Bedworth and independently by Tammann.[14,15] The derivation is based on the solid state diffusion of ions in an oxide film. The concentration of diffusing atoms or ions is assumed linear and inversely proportional to the thickness. An adherent oxide layer has to be formed in order that the parabolic rate law be applicable. The parabolic rate law may not apply until a certain thickness of film is developed. The phenomena causing the deviation were expressed by Kubaschewski and Hopkins as follows:

(1) the effect of the decrease in roughness or surface area as the reaction proceeds

(2) the effect of the heat evolved in the reaction on the rate of reaction

(3) the effect of the solution of oxygen in the metal on the rate of reaction

(4) the effect of the concentration of impurities in the oxide during the early stages of the reaction

(5) the change in oxide composition, and

(6) the influence of potential fields at the gas interface due to adsorbed oxygen ions ...[16]

Phelps, Gulbransen, and Hickman showed that deviations could occur because lateral growth of crystals starts at scattered nuclei and lateral growth occurs as well as vertical growth until a complete layer is formed.[17]

The logarithmic rate law has been found applicable in several cases and various theories and derivations have been proposed. The determining factors are apparently quite complex and present one of the many unsolved problems in the study of metal surface oxidation.

Factors Affecting the Rate of Oxidation. The main factors affecting the mechanism of oxidation of a metal are temperature, pressure, surface condition, purity of the metal and gases, and the physical properties of the oxide or oxides.

Temperature affects the oxidation process in many ways. The rate of the chemical reaction between the metal and the oxygen is dependent on temperature as well as the rate of diffusion of ions of one or both of the reactants through the oxide layer. The diffusion process in nickel oxide is considered to be a flow of nickel ions accompanied by electronic flow.[18] Diffusion of ions and chemical reaction at the interface are the two major steps in the oxidation process. The step determining the rate of oxidation will be the step with the larger activation energy. Elevated temperatures may

cause the oxide to volatilize or to crack due to stresses set up by differential expansion of the metal and the oxide. With certain metals, such as iron and cobalt, temperature controls the composition of the oxide or oxides formed. Nickel has been found to form only one oxide, NiO, in the range of 450° - 700° C., but Ni_3O_4 has been reported at lower temperatures.[9] Experimental results of Finch and Sinha indicated the possible formation of a spinel of the composition $Ni_{28}O_{32}$ but the existence of such a spinel has not been firmly established.[19]

The oxygen pressure may have an influence on the rate of reaction in at least two situations. If the rate of oxidation is controlled by the rate of reaction at the interface between the oxide and oxygen, the pressure of the oxygen may influence the rate of oxidation. Also the amount of oxygen dissolved in the metal would be dependent on the oxygen pressure and dissolved oxygen may cause a definite change in the rate of oxidation. Oxygen pressures of 7.6 cm mercury and 10 cm mercury have been found sufficient to make the rate constant independent of pressure for the oxidation of nickel and dependent on the diffusion of nickel through the oxide film.[1,7] The oxygen pressures used in this investigation were high enough for the rate of oxidation to be independent of pressure.

Comparison of results of various investigators, especially for thin films, has often been found difficult due to different surface conditions. Methods of sample preparation may vary from very tedious methods to merely degreasing the sample with a suitable solvent. Different methods of sample preparation give different degrees of roughness which causes a wide range in the important ratio of true surface area to apparent geometric surface area. This ratio

is especially important when thin films are being studied. Another factor to be considered is the nature of the surface produced by the reduction of an oxide. The reduced oxide will give a surface of high energy condition and a high ratio of true surface area to geometric surface area. The procedure adopted for sample preparation in this investigation was selected because it was a simple method which should give consistent results. The ratio of true surface area to geometric surface area was assumed to be unity for this investigation.

The importance of purity of the metals used for oxidation investigations on "pure" metals has often been neglected. The comparison of results between different investigators has often been impossible due to insufficient information concerning the purity of the metal used. The effect of purity on oxidation of nickel has previously been discussed. Kubaschewski and Hopkins state that the effect of impurities can rarely be predicted but impurities chemically similar to the basic metal have much less effect than those chemically different.[20] They also state that the amount of the latter type of impurity should be kept well below 0.01%. The consideration of the effect of alloying elements is considered too extensive to be included in this report.

Impurities in the gaseous atmosphere may be as important as impurities in the metal. Gaseous impurities, including inert gases, may be preferentially adsorbed or have adsorptive properties that affect the adsorption of the oxidizing gas.[21] Foley and Guare found the rate constant for the parabolic rate law varied as much as 60% for similar runs conducted in laboratory air on different days and oxygen-nitrogen mixtures gave much more reproducible results.[22]

When using air, the effect of nitrogen must be considered. A nitride of nickel does exist but it decomposes rapidly at temperatures as low as 440° C.[23] It has been assumed in this investigation that a negligible amount of nitride would exist at the elevated temperatures. The solubility of oxygen in nickel is 0.012% at 1200° C. and increases with decreasing temperature.[24] Degassing the samples would remove part of the gases in solid solution in the metal but the temperature used for degassing should cause the major portion of the dissolved oxygen to combine and form the oxide internally.

The physical properties of the oxide or oxides formed affect the degree of protection from further oxidation. For many years it was generally agreed that the oxide would be porous when the ratio of the specific volume of the oxide to the specific volume of the metal oxidized was less than unity. Many investigators still follow this idea but Gulbransen stated in 1949 that the ratio is probably not too important since the oxide crystals can grow only in one direction and the ratio would only determine the relative thickness of the film.[25] The plasticity of the oxide determines the ability of the oxide to follow the residing metal surface when growth occurs at the oxide gas interface.

Nickel oxide has a slightly distorted NaCl structure.[18] The rate of diffusion of nickel is dependent on the concentration of vacant Ni^{+2} sites or Ni^{+3} ions as shown in Figure 4. Moore and Lee stated that the concentration of excess oxygen or vacant Ni^{+2} sites in nickel oxide is about 3×10^{-3}%.[26]

$O^{=}$	Ni^{++}	$O^{=}$	Ni^{3+}	$O^{=}$
Ni^{++}	$O^{=}$	Ni^{++}	$O^{=}$	Ni^{++}
$O^{=}$	Ni^{3+}	$O^{=}$	$\square$	$O^{=}$
Ni^{++}	$O^{=}$	Ni^{++}	$O^{=}$	Ni^{++}

Figure 4. Metal deficit structure of nickel oxide.[26]

III. EQUIPMENT AND PROCEDURE

Equipment. Figure 5 is a picture of the apparatus with the exception of the cathetometer and the constant-temperature water bath. A corner of the latter is shown on the left in the picture. Figure 6 is a simplified block diagram of the experimental apparatus. The Leeds and Northrup Speedomax Type H controller maintained a constant temperature in the reaction zone within ±2° C. using a thermocouple attached to the outer surface of the mullite reaction tube. The controller was adjusted so as to have the desired temperature in the mullite tube as measured with a thermocouple and potentiometer. The platinum-wound Marshall furnace was adjusted with a shunt so as to have a four-inch zone of constant temperature in which to locate the sample.

The furnace was mounted on rails so it could be brought to temperature and then moved onto the reaction tube. The sample could then be inserted and the system evacuated while the furnace was attaining the desired temperature.

A vacuum tight mullite to pyrex seal connected the mullite reaction zone to the rest of the apparatus. The precision-bore pyrex tube in which the mercury indicator moved had an inner diameter of 0.1250 ± 0.0002 inches. Vacuum stopcocks with a silicone lubricant were used at the two necessary points shown on the block diagram. Silicone lubricant was also used on the ground joint used for sample entrance into the reaction zone.

The freeze traps in series were filled with glass beads for more contact area and therefore complete drying of the gas. They were maintained at -79° C. with acetone and dry ice. Copper foil at 600° C.

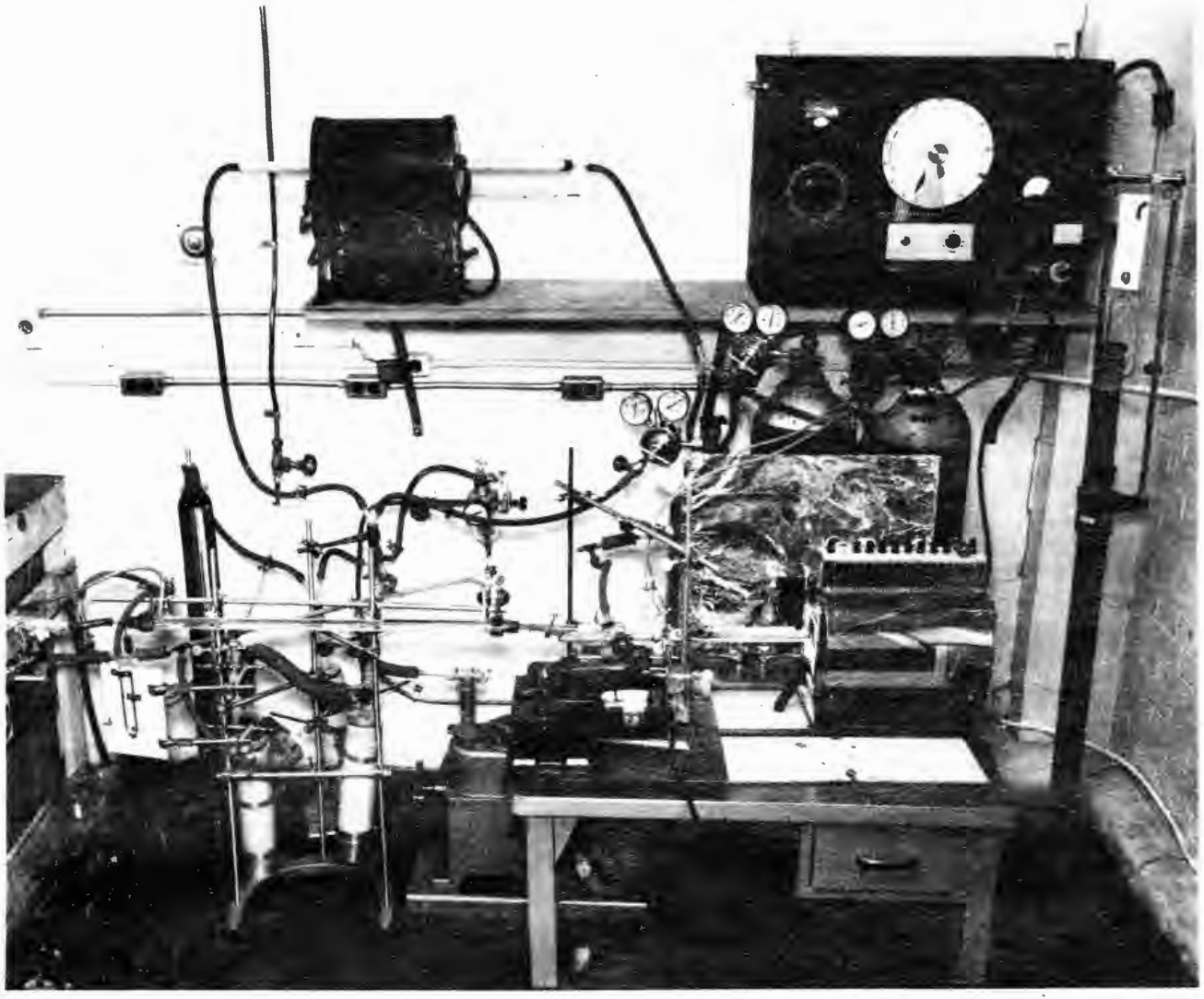

Figure 5. – Volumetric Apparatus.

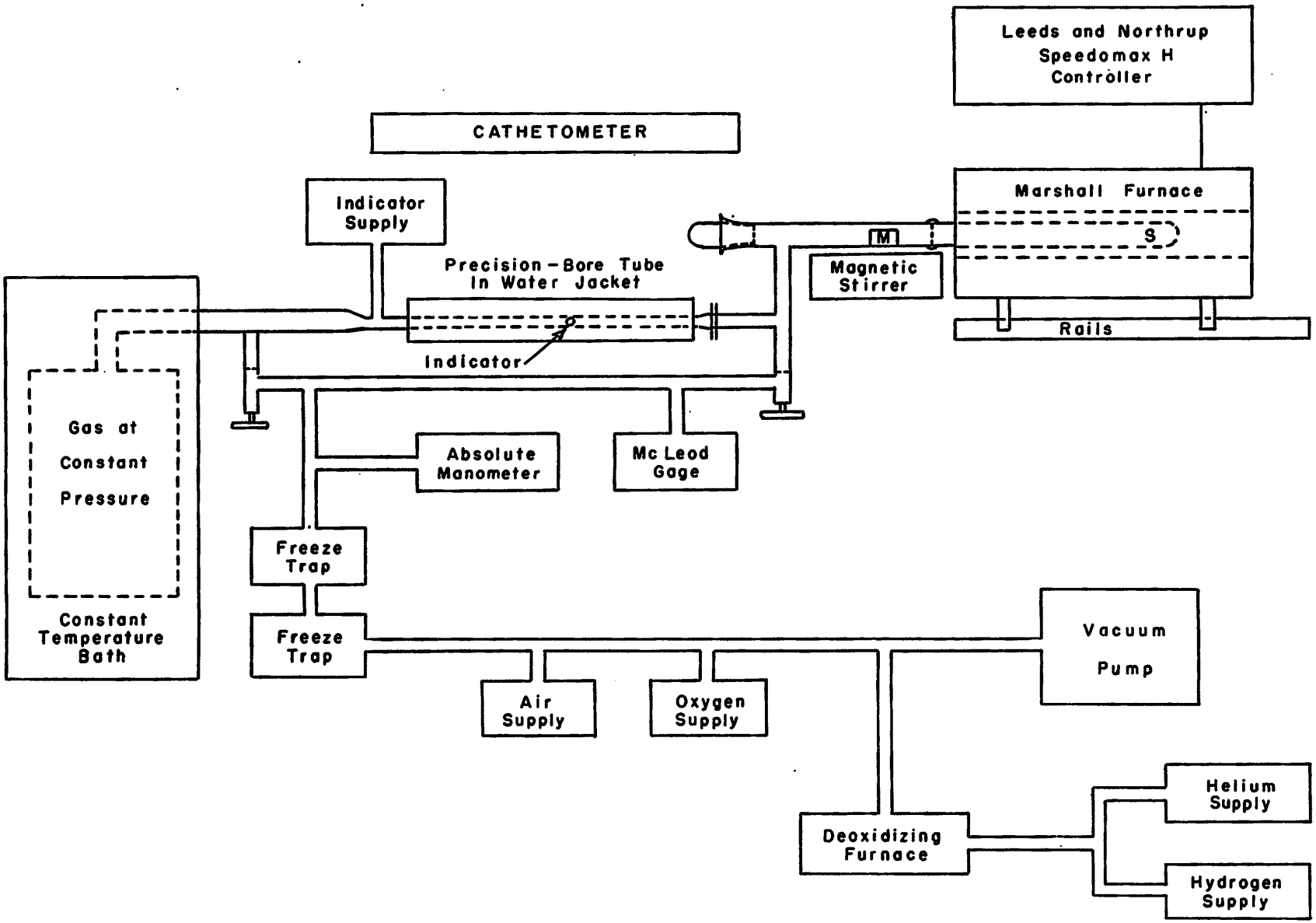

Figure 6. – Volumetric Oxidation Apparatus.

F-1265-RO

was used in the deoxidizing furnace to remove possible traces of oxygen from the high-purity helium. The copper foil was rejuvenated periodically by reducing the oxide with hydrogen at 600° C.

The large constant-pressure reservoir was a five gallon pyrex bottle with a connecting elbow on the top. The elbow was made as one unit with the bottle. A 60 pound lead plate was fastened to the bottle to prevent floating in the constant-temperature water bath. The water bath was actually two separate baths with one inside the other. Each unit functioned separately with its own mercury thermoregulator, knife-edge immersion heater, and stirrer. The constant-temperature baths were enclosed in a wooden box with approximately three inches of excelsior packed around the outer metal container for insulation. The temperature was maintained constant to $\pm 0.1°$ C. A sigma pump maintained a constant flow of water through the water jacket on the precision-bore tube from the inner unit of the water bath. The precision-bore tube, and therefore the gas in the tube, was maintained at 34° C.

A magnetic stirrer was used when air instead of pure oxygen was employed for a run. The magnetic stirrer consisted of two parts. One part was a small magnet encapsulated in one inch of pyrex tubing (outer diameter - 0.8 cm) which was inside the pyrex portion of the reaction chamber. The other part was a magnet on a block of wood which was gradually moved back and forth below the pyrex portion of the reaction chamber on two steel rods by an eccentric arm on a gear. The gear was rotated at a reduced speed by a gear reducer on an electric motor. The encapsulated magnet moved at a rate which displaced five cm^3 of gas per minute. The purpose of the magnetic stirrer was to reduce the effect of thermal diffusion which would tend to cause the

heavier component, oxygen, to concentrate in the cold end of the reaction chamber while the nitrogen increased in concentration in the hot reaction zone.

Figure 7 is a simplified drawing with (V) the constant-pressure reservoir and (v) the reaction chamber.[3] The pressure in the reaction chamber would decrease as oxygen was used up in the oxidation process. The indicator would then be moved toward the reaction chamber by the constant pressure in the large reservoir. The volume of the reaction chamber was 75 cm^3 and the volume of the constant-pressure reservoir on the other side of the indicator was about 21,000 cm^3. This gave a ratio of volumes of 1:280. The volume in the reaction chamber changed about 4 cm^3 during the movement of the indicator from one end of the measuring zone to the other before its movement was reversed. A 5 percent change, or 4 cm^3, in volume in the reaction chamber would be accompanied by a 0.019 percent change in volume in the constant-pressure reservoir which would have a negligible effect on pressure.

Procedure. Nickel of three different purities was investigated at 1200° C. to check the effect of purity on the rate of oxidation and also to determine the applicable rate law. Investigations were also conducted on nickel of the highest purity available at 1300° C. The composition of the sheet nickel is given in Table I.

The samples were cut from the nickel sheets with stainless steel scissors. Scrap nickel was cut with the scissors prior to cutting samples so as to clean the scissors and reduce contamination. The samples were approximately 0.02 cm thick and ranged in total area from 1.5 cm^2 to 4 cm^2.

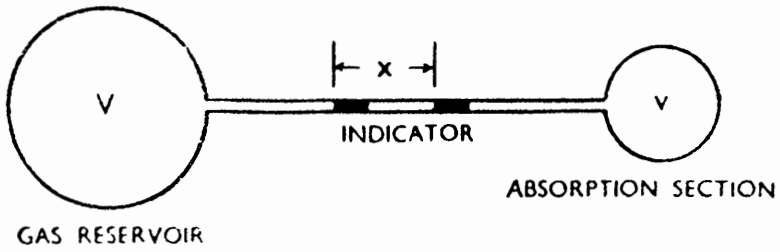

Figure 7. Schematic representation of the volumetric oxidation apparatus.[3]

Table I

Foundry Nickel (Produced from cast Ni)	National Lead Nickel (Produced from powder)
0.55% Co	0.11% Co
0.04% Fe	0.007% Fe
0.23% Mn	0.0005% Mn
0.006% Cu	less than 0.001% S
0.001% S	

INCO HPM Nickel (Produced from powder)

0.002% Co

0.006% Fe

less than 0.001% S

AIRCO Oxygen	USBM Helium
99.5% O_2	99.995% He

The samples were all subjected to the same sample preparation prodedure prior to oxidation so as to minimize possible variables. Each sample was polished through 4/0 emery paper and cleaned with acetone. The procedure for bright annealing nickel was followed and the samples were annealed in hydrogen for 20 minutes at 770° C.[27] The samples were stored in a dessicator until needed.

The sampled holders were short pieces of quartz or porcelain tubes. The quartz was used for runs at 1200° C. and the porcelain was used at 1300° C. The sample size was adjusted so that the samples would support themselves near the center of the tubes. The contact of the edges of the samples with the tube would slightly reduce the rate of oxidation on the edges. The oxidation rate at the edge would not be the true rate found in the bulk of the sample but the amount of area affected was negligible compared to the total area of the sample. It was also assumed that a negligible amount of silicon would diffuse into the sample. The samples were found to be free to move after oxidation so it was assumed that no stresses were developed by expansion of the sample during oxidation which would cause cracking of the oxide or other indeterminent effects.

Prior to starting a run, the freeze traps were charged and the furnaces and constant-temperature bath brought to operating temperature. The sigma pump was also turned on to bring the water in the water jacket on the precision-bore tube to temperature. The procedure used was then as follows:

(1) The sample holder and the weighed and measured sample were inserted in the reaction chamber.

(2) The system was evacuated to a pressure of 50 microns of mercury.

(3) The system was filled to a pressure of 60 centimeters of mercury with dried deoxidized helium and again evacuated to a pressure of 50 microns of mercury. This step was repeated if the system initially had not been filled with helium when it was opened and the sample inserted.

(4) The reaction chamber was shut off from the rest of the system by closing the vacuum stopcock and also a pinch-cock on the short piece of thick-walled rubber tubing connecting the reaction zone to the precision-bore tube.

(5) The furnace, which was at or near operating temperature, was moved gradually along the rails onto the reaction zone.

(6) The reaction zone and sample were maintained at or near operating temperature in the vacuum for about 2.5 hours to degas the sample and to reduce the amount of adsorbed gases on the mullite tube.

(7) Oxygen or air was introduced into the system to the desired pressure with the reaction chamber still sealed off in a vacuum. The magnetic stirrer was turned on if air was being used.

(8) The timer was started and the reaction chamber was opened to the rest of the system to admit air or oxygen.

(9) The two vacuum stopcocks were closed and gas added to the indicator reservoir, which was a U-tube, until a drop of mercury was forced up into the precision-bore tube.

(10) A small amount of gas was added to the reservoir side of the system to free the drop of mercury from the column in the U-tube and place it in the section of precision-bore tube enclosed by the water jacket. At this time the pressure in the reservoir, and therefore in the reaction chamber, was carefully checked with the absolute manometer.

(11) The movement of the indicator in the precision-bore tube was followed with the cathetometer and readings were taken periodically.

(12) After the indicator had traveled the complete length of the precision-bore tube, the indicator was returned to its initial position to allow continued measurement. This was done by slightly opening the vacuum stopcock on the reaction chamber and adding dried oxygen. Only oxygen was added since only oxygen was being consumed even when air was used for the run. The reversal of the indicator by adding oxygen kept the oxygen concentration and the pressure in the reaction chamber approximately constant.

(13) At the end of the run oxygen was added to the reaction chamber until the indicator moved back and fell into the indicator reservoir. The gas pressure behind the mercury in the U-tube reservoir was then adjusted so as to be equal to the pressure in the rest of the system.

(14) The system was evacuated with the vacuum pump and the furnace moved back on its rails off the reaction zone as fast as it was judged the mullite tube could stand the thermal shock. At this rate it normally took two minutes to move the furnace off the mullite tube and then about four minutes more for the mullite tube to cool to a temperature where further oxidation would be negligible.

(15) The system was filled with helium and the sample removed and weighed and a new sample inserted.

The volume through which the indicator moved was converted to mg of oxygen consumed per cm^2 of sample by the oxidation reaction. The temperature of the gas in the precision-bore tube was maintained at 34° C. by the water jacket and the pressure was determined by the absolute manometer. Oxygen was considered as an ideal gas for the

conversion from volume to weight. The geometric surface was used for all calculations and no attempt was made to determine the true surface area. The measured weight gain was obtained with a balance sensitive to 0.1 mg so each measured weight gain would be accurate to ± 0.2 mg. The weight loss due to sublimation of the metal or oxide was neglected in all calculations.

Experimental Errors. The main errors possibly introduced by the apparatus and procedure may be grouped into two main categories, indeterminant volume change periods, referred to as lost time, and contamination.

There were three periods during which it was impossible to measure the amount of oxidation. The data for these periods were estimated from the rate before and after the lost time. At the start of the run about two minutes were normally lost during the adjustment of the pressure and introduction of the indicator. A similar amount of time was lost during each reversal of the indicator. At the end of each run the indicator was reversed and returned to the indicator reservoir. The system was then rapidly evacuated and cooled to room temperature. An estimate of the oxidation during evacuation and cooling was necessary but it was usually a relatively small amount due to the slow rate of oxidation with the thick oxide film present.

The contamination of the gaseous environment in the reaction chamber may have come from three main sources. The mercury indicator could introduce a small amount of vapor since the vapor pressure of mercury at 34° C. is 3.8×10^{-3} mm of mercury. The surface area of the indicator was quite small and the diffusion of the heavy mercury atoms would be quite slow through the small precision-bore tube. The greater part of the mercury vapor would oxidize before it reached

the sample but this would then affect the amount of oxygen consumed. Attempts were made to use diffusion pump oils, such as di-butyl phthalate, for the indicator. The oils had lower vapor pressures than mercury but they wet the walls of the precision-bore tube and gradually dispersed while moving through the tube. The silicone stopcock lubricant had a vapor pressure of 10^{-8} mm of mercury and a very small exposed area. It would also tend to oxidize as the vapor entered the reaction zone. The other possible source of contamination was the sample. Carbon, sulfur, and other impurities may form volatile contaminants and affect the reaction at the metal surface and also the amount of oxygen consumed. This imposes a limitation on the use of the volumetric technique. Only metals or alloys should be used that are relatively free of such contaminants. The vapor of the metal or the oxide may also become an important factor at elevated temperatures. The vapor pressure of nickel and nickel oxide at 1200° C. is respectively about 4×10^{-8} atmospheres and 1×10^{-8} atmospheres.[28]

A great deal of trouble was encountered in the initial tests due to adsorbed or entrapped gases in the mullite tube. The amount of gas released and affecting the run decreases with consecutive runs due to the crystal size of the mullite increasing and reducing the surface area. The gas released often amounted to over 1 cm^3; consequently, it was necessary to add a bake-out period at an elevated temperature prior to adding oxygen and starting the run.

After the initial pressure difference necessary to overcome the inertia of the mercury indicator had been established, it was calculated that the apparatus was sensitive to 0.01 mg.

IV. RESULTS

Data. The data for the experimental runs are tabulated in the Appendix. Three runs were carried out for each set of conditions investigated. The rate of oxidation was measured at 1200° C. for INCO HPM nickel, National Lead nickel, and Foundry nickel. It was also measured at 1300° C. for INCO HPM nickel.

Correlation with the Parabolic Rate Law. After an initial period of deviation, the oxidation of nickel at 1200° C. and 1300° C. for three hours followed the parabolic rate law. Figure 8 is a parabolic plot of the averaged data for each set of conditions investigated. Ideally, all points would fall on straight lines.

When data which fit the parabolic rate law equation are plotted as the log of the weight gain versus log of time, the slope of the straight line through the points is 0.50. Figure 9 is a log-log plot for the averaged data for each set of conditions investigated. The slope of the straight line for points after 40 minutes of elapsed time for each run and for the averaged data for each set of conditions was calculated by the method of least squares. The slopes are reported in Table II. The constant, K, for the parabolic rate law equation and the average grain size of the nickel remaining after oxidation are also reported in Table II.

Effect of Temperature and Purity. Figure 10 shows the effect of 100° C. difference in temperature on INCO HPM nickel by showing weight gain versus time for the averaged data for 1200° C. and 1300° C. Figure 10 also shows the effect of purity on the rate of oxidation of nickel at 1200° C.

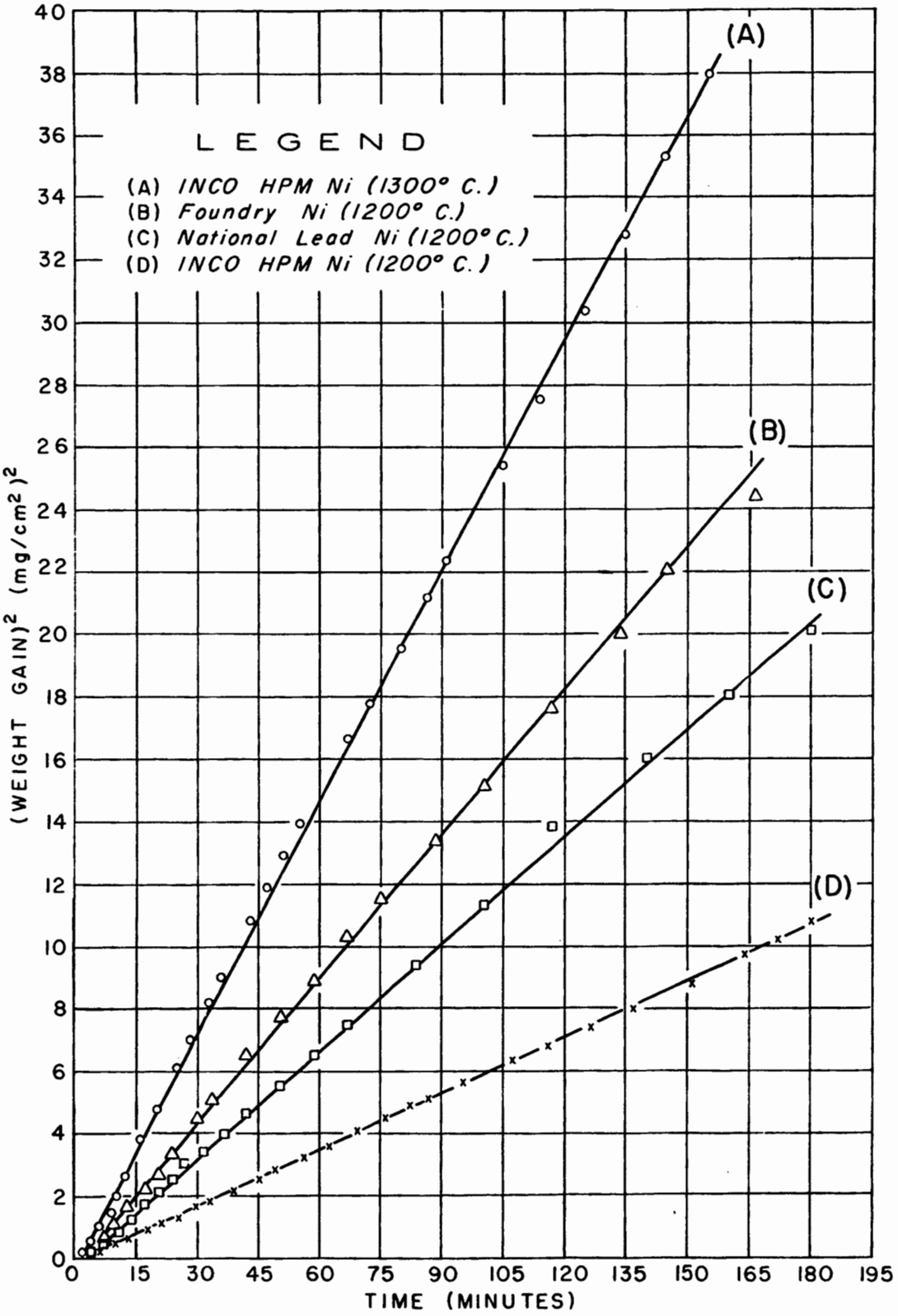

F-1280-RO

Figure 8.- Parabolic Plot

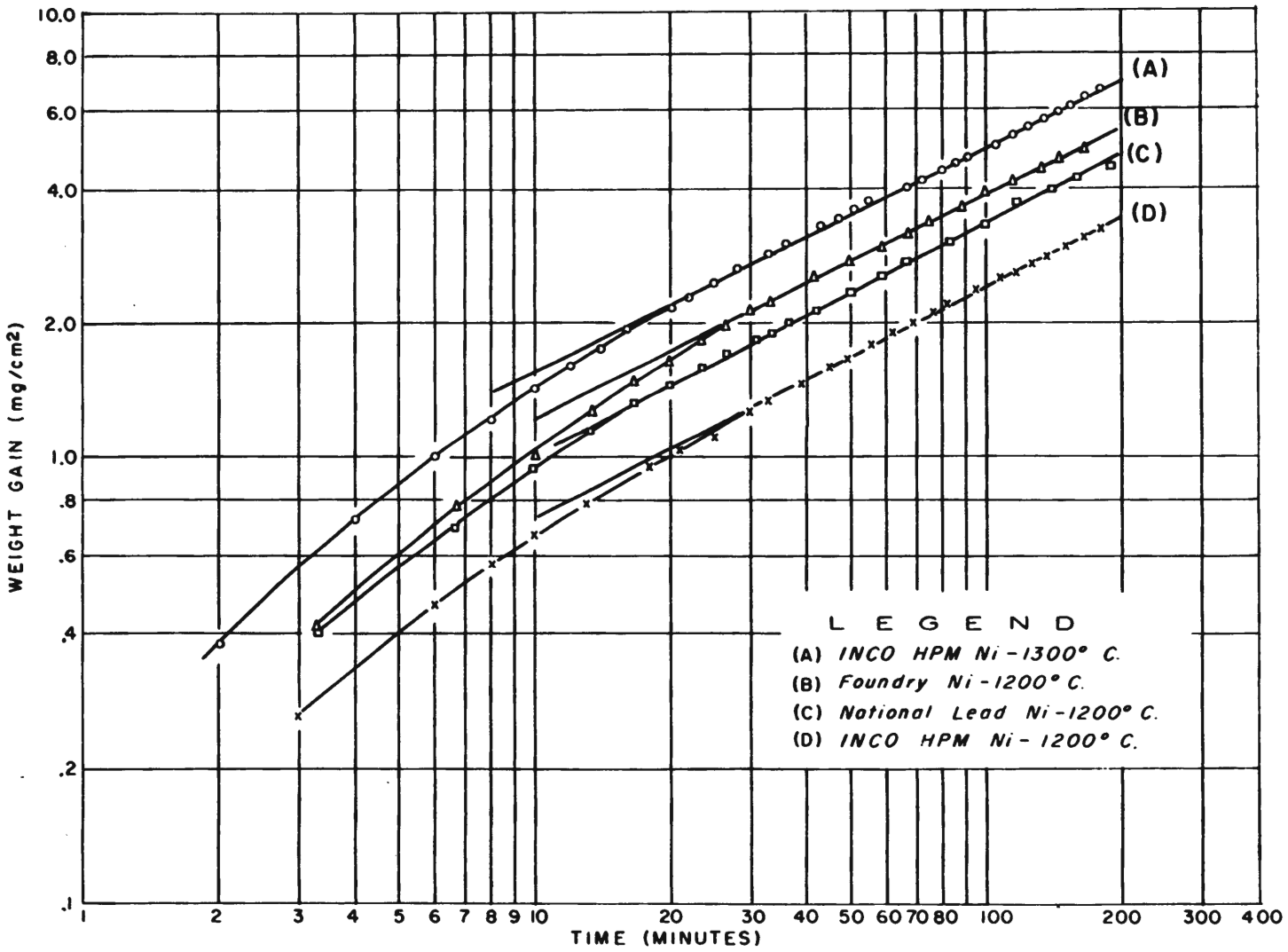

Figure 9.- Weight Gain Versus Time (Log-Log)

F-1281-RO

Table II

Run	Log-Log slope 0.50 ≒ parabolic	$W^2 = Kt$* K	Grain Size After Oxidation
F-11	0.468		
F-12	0.472		
F-13	0.541		
Average data for National Lead Ni(1200°)	0.511	0.113	0.9 mm
F-14	0.483		
F-15	0.447		
F-16	0.467		
Average data for Foundry Ni (1200°)	0.480	0.152	0.9 mm
F-24	0.509		
F-26	0.504		
F-27	0.478		
Average data for INCO HPM Ni (1300°)	0.489	0.246	0.15 mm
F-28	0.502		
F-29	0.491		
F-30	0.543		
Average data for INCO HPM Ni (1200°)	0.510	0.593	0.12 mm

* W-(mg/cm^2); t-(min.)

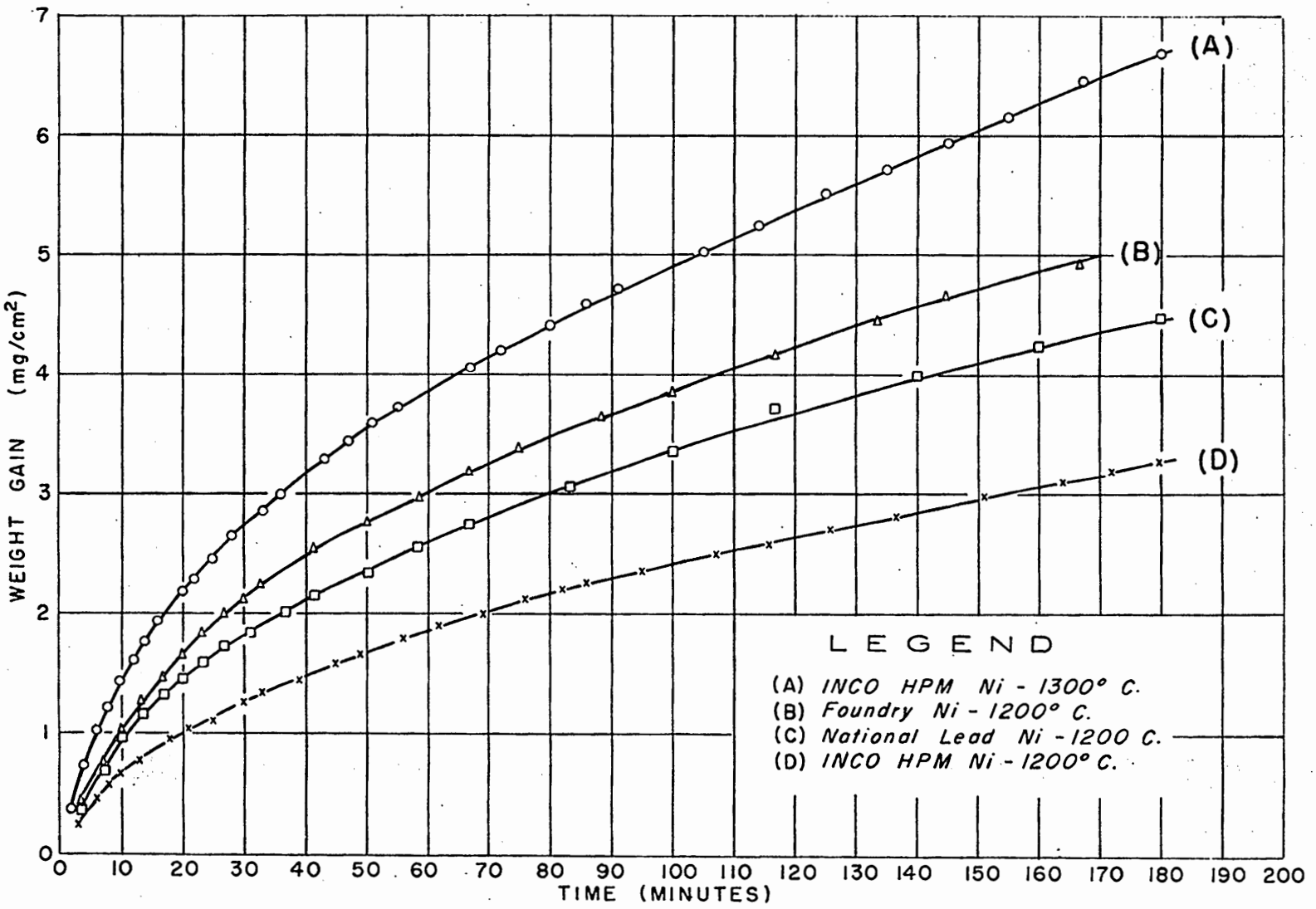

Figure 10.- Weight Gain Versus Time

F-1282-RO

The impurities may affect the amount of internal or subsurface oxidation. No visible internal oxidation was observed in the INCO HPM nickel in the etched or unetched condition. Figure 11 and Figure 12 show what may possibly be internal oxidation in National Lead nickel and Foundry nickel.

Figure 13 shows etch pits formed by thermal etching during growth of the oxide. Etch pits occur at dislocations and the number of dislocations would be related to the purity of the oxide. The etch pits were prevalent in the oxide on Foundry nickel with a much smaller number in the oxide on National Lead nickel and very few in the oxide on INCO HPM nickel. The most interesting examples of etch pits were observed on two samples of nickel oxidized in room air for 60 days at 1200° C. The nickel was similar in purity to Foundry nickel and contained 0.67% Co, 0.01% Fe, 0.003% Cu, 0.007% Si, and less than 0.001% S. Figure 14 and Figure 15 show some of the smaller, but most interesting, etch pits on this nickel.

Activation Energy. The activation energy for the process controlling the rate of oxidation of INCO HPM nickel was calculated for the range of 1200° - 1300° C. using the Arrhenius equation. An activation energy of 40,700 cal/mole was obtained by assuming a straight line for the plot of log K versus 1/T between 1200° C. and 1300° C. The agreement with the activation energy reported by other investigators is shown in Table III.

Reproducibility of Results. Table IV shows the agreement between the measured weight gain of the samples and the weight gain calculated from the measured volume of oxygen consumed in the oxidation reaction. The balance used to measure the weight gain was sensitive to 0.1 mg so each measured weight gain could then be considered accurate to

Figure 11. Possible internal oxidation in National Lead Ni oxidized at 1200° C. Sample F-20, unetched, 500X.

Figure 12. Possible internal oxidation in Foundry Ni oxidized at 1200° C. Sample F-14, unetched, 500X.

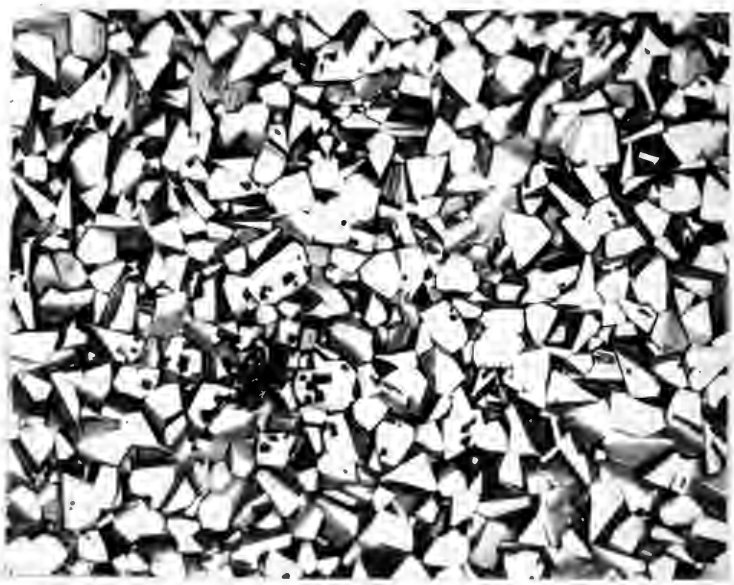

Figure 13. Etch pits in nickel oxide on Foundry Ni oxidized at 1200° C. Sample F-16, unetched, 500X.

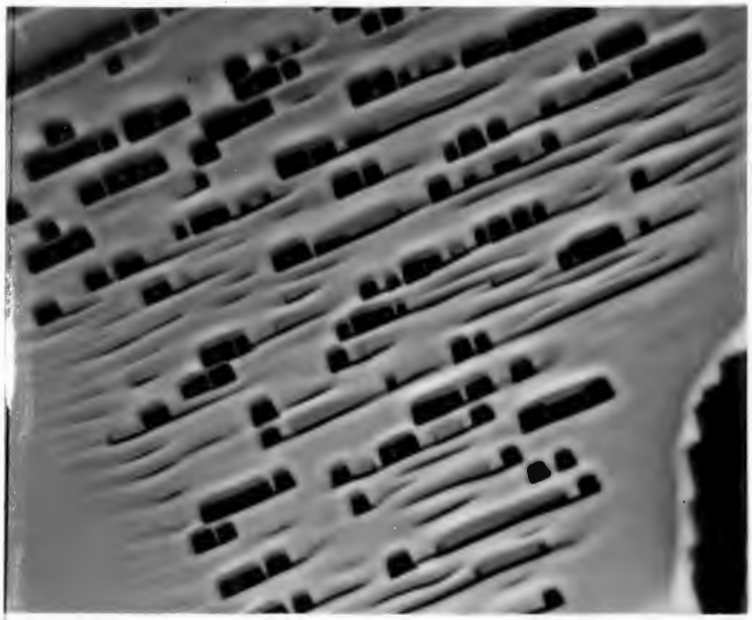

Figure 14. Etch pits in nickel oxide on low purity nickel oxidized at 1200° C. for 60 days. Unetched, 2000X.

Figure 15. Etch pits in nickel oxide on low purity nickel oxidized at 1200° C. for 60 days. Unetched, 2000X.

Table III

Investigator	Temperature	Activation Energy (cal/mole)
Friebel	1200° - 1300° C	40,700
Gulbransen and Andrew[1]	up to 900° C	41,200
Gulbransen and Andrew[1]	over 900° C	68,300
Moore and Lee[7]	400° - 900° C	38,400
Kubaschewski and Hopkins[29]	400° - 1000° C	34,700
Shim and Moore[30]	1000° - 1400° C	44,200*

*Activation energy for the diffusion of nickel in monocrystalline and polycrystalline NiO while the others are for the oxidation of nickel.

Table IV

Run	Temperature (°C)	Weight gain calculated from measured volume of oxygen consumed (mg)	Measured weight gain (mg)
F-11	1200°	11.8	12.0
F-12	1200°	14.2	14.0
F-13	1200°	9.9	10.0
F-14	1200°	11.6	11.9
F-15	1200°	14.3	13.8
F-16	1200°	12.7	12.6
F-24	1300°	9.6	9.2
F-26	1300°	24.0	23.1
F-27	1300°	17.6	16.6
F-28	1200°	13.8	13.9
F-29	1200°	14.2	14.4
F-30	1200°	13.1	—

±0.2 mg. At 1300° C. the measured weight gain was 4-6% lower than the weight gain calculated from the volume of oxygen consumed. A sample was scraped from the inside of the mullite reaction tube in the region which extended from the furnace during the runs. A spectrographic analysis showed nickel present in the sample.

Figure 16 shows the agreement between runs on National Lead nickel at 1200° C. in oxygen. The vertical displacement of the curves shows a small amount of variance but the curvature is in close agreement between runs.

Figure 17 shows the agreement between runs on Foundry nickel at 1200° C. in air. The vertical displacement is quite small with good agreement in curvature for two runs and a definite deviation for the other run.

Figure 18 shows the agreement between runs on INCO HPM nickel at 1200° C. in oxygen. The small vertical displacement and the curvature show the excellent agreement between the runs on the high-purity nickel.

Figure 19 shows the agreement between runs on INCO HPM nickel at 1300° C. in oxygen. The curvature is in fair agreement but the vertical displacement shows considerable variation between runs.

Oxide Properties and Structure. The oxide was adherent to the nickel at the completion of all runs and was uniform and free of imperfections such as blisters. No spalling of the oxide occurred during any runs or upon rapid cooling to room temperature. The oxide on the samples referred to in the section on Effect of Temperature and Purity, which were oxidized for 60 days at 1200° C., was still uniform and adherent to the nickel. It was also free of visible cracks after being air quenched from 1200° C. to room temperature. Figure 20 shows the only

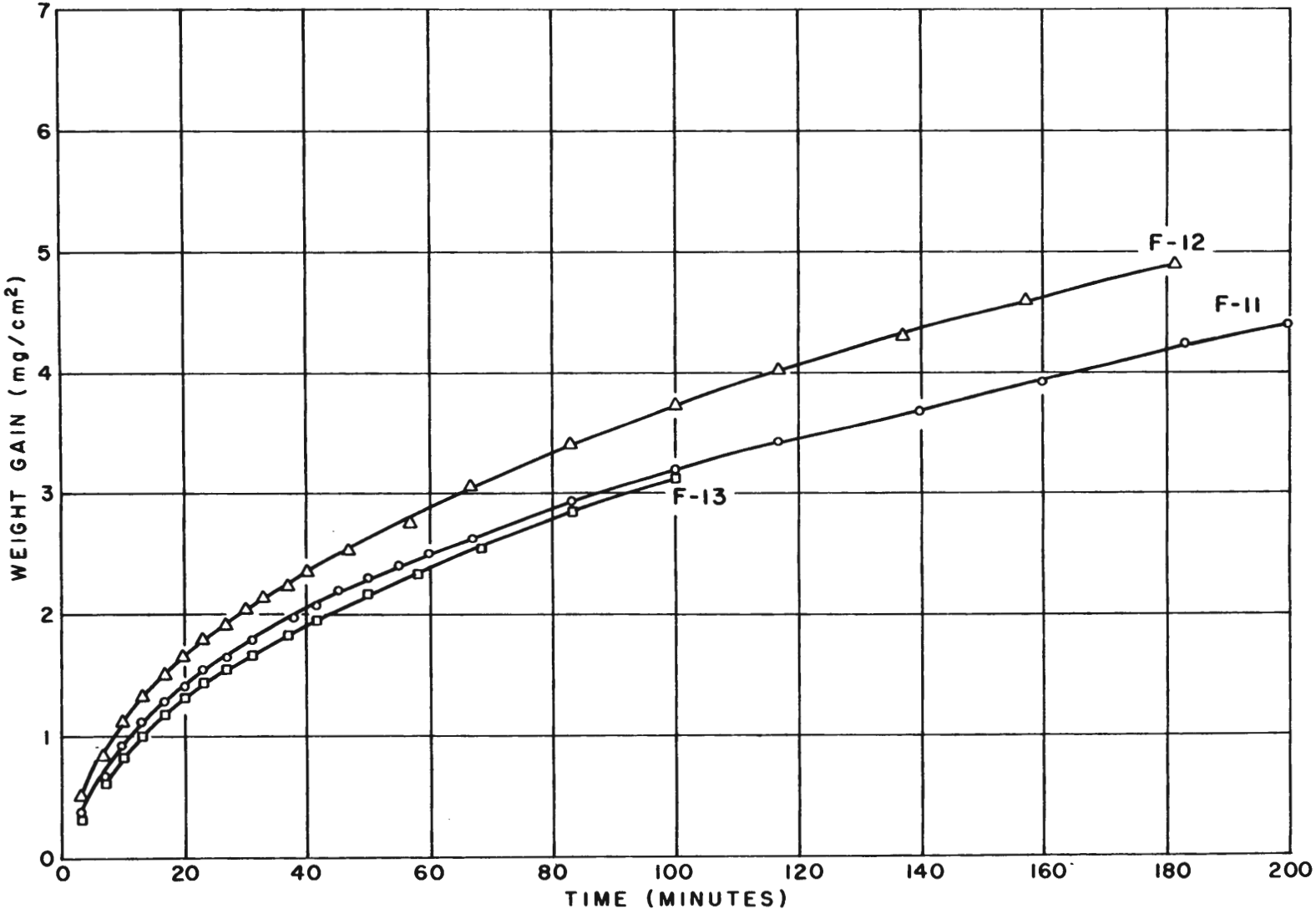

Figure 16.- National Lead Nickel 1200 Degrees C.- Oxygen.

F-1283-RO

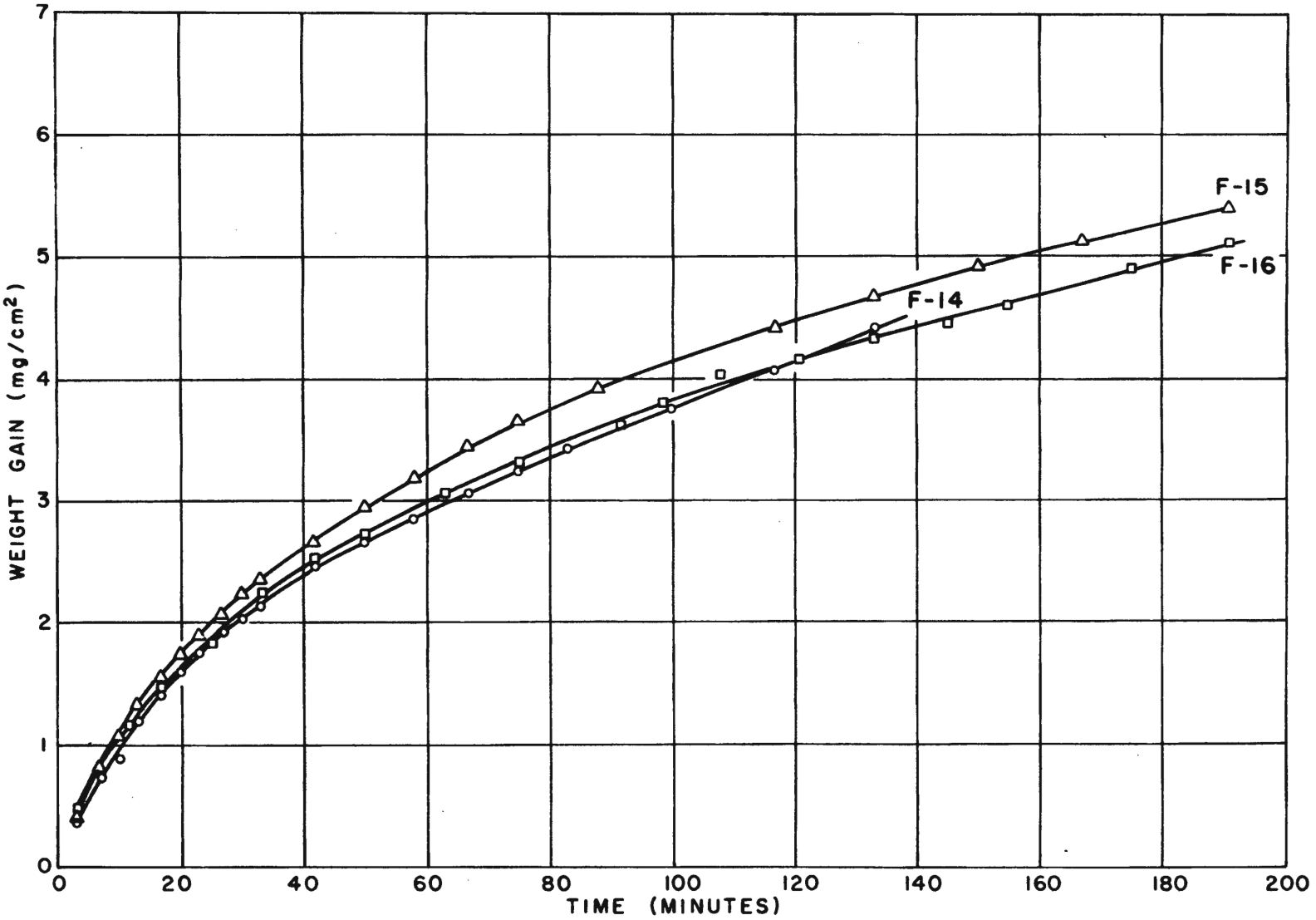

Figure 17.- Foundry Nickel 1200 Degrees C. - Air.

F-1284-RO

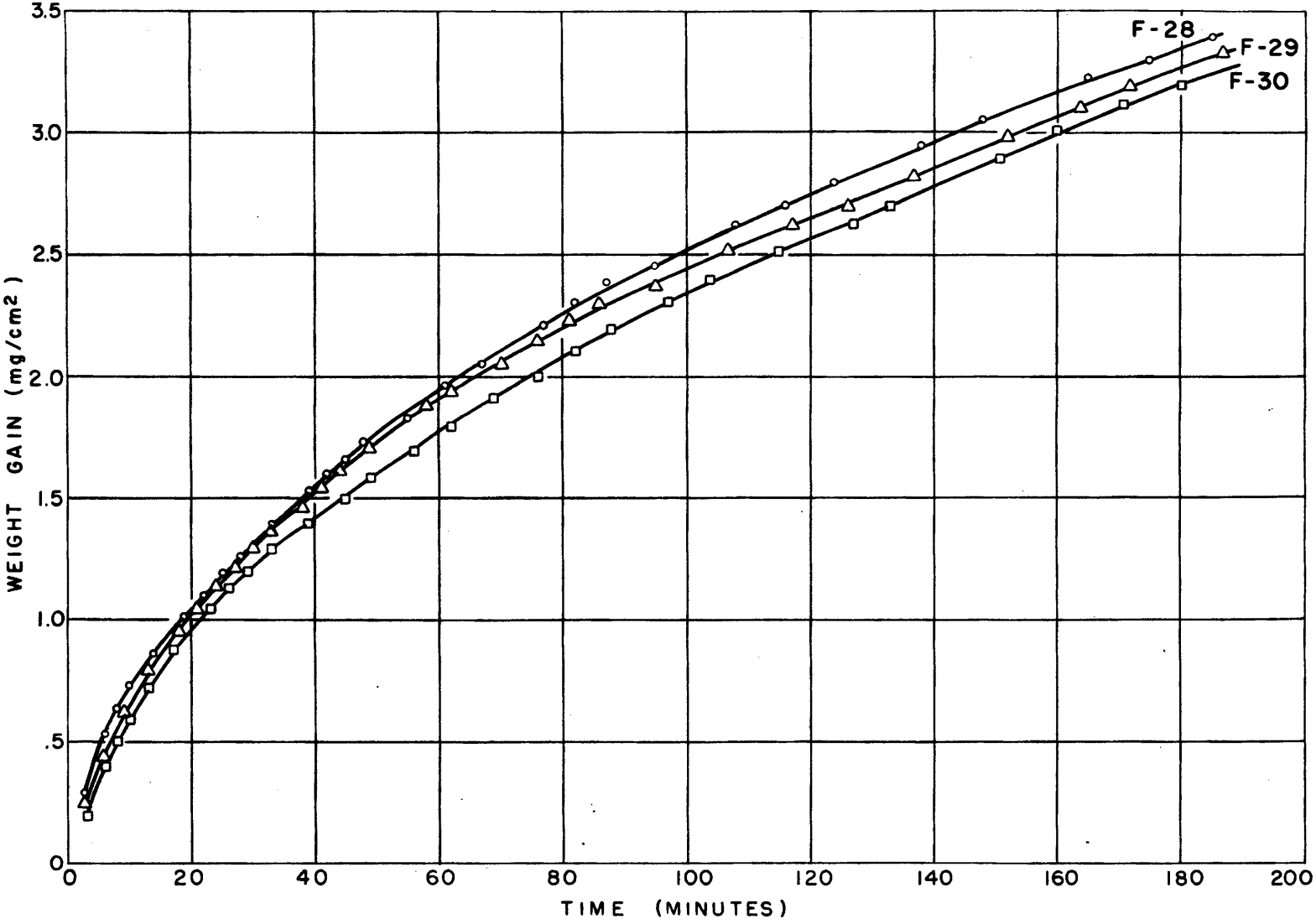

Figure 18.- INCO HPM Nickel 1200 Degrees C. – Oxygen.

F-1285-RO

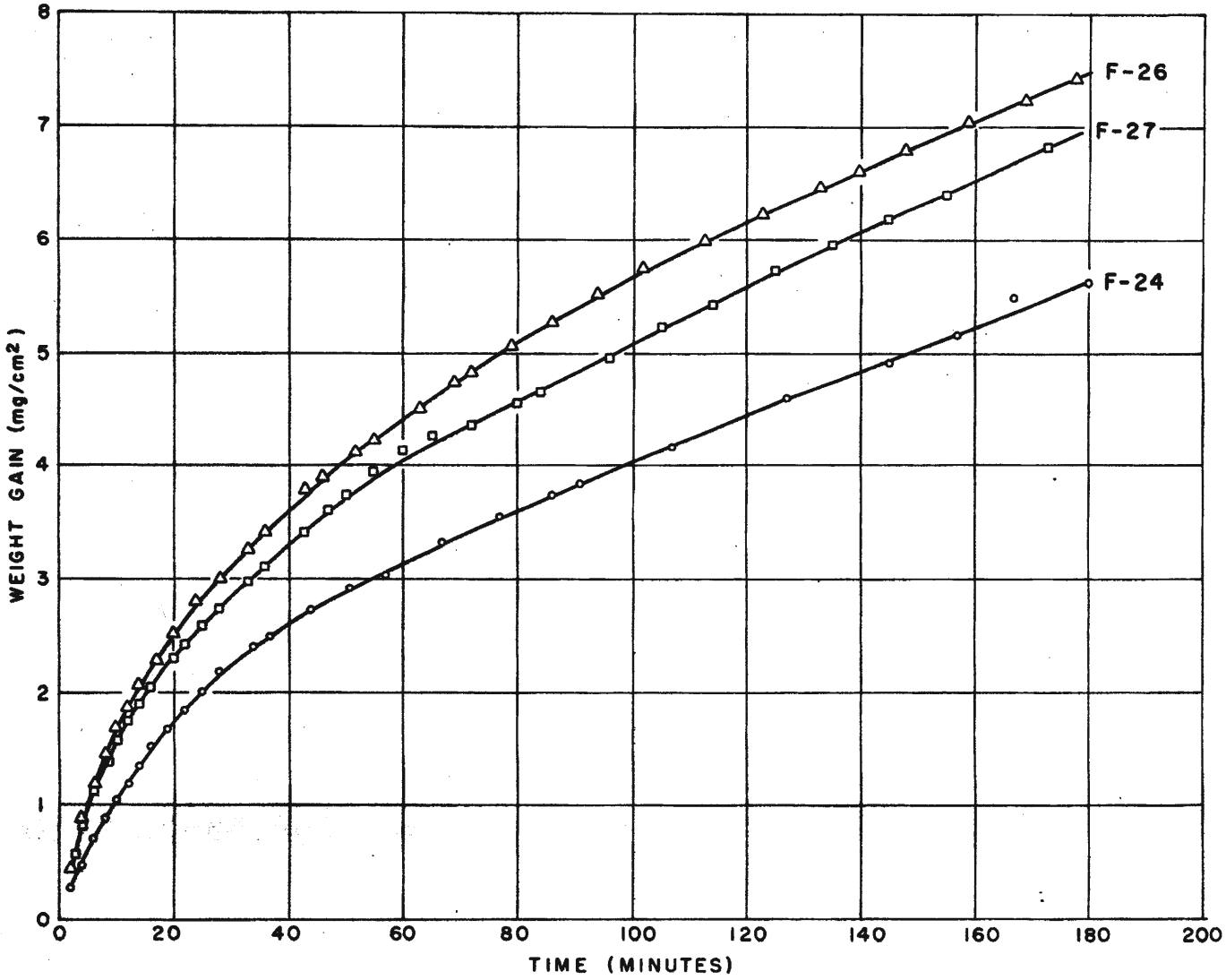

Figure 19.-INCO HPM Nickel 1300 Degrees C. - Oxygen.

F-1286-RO

Figure 20. Cracked nickel oxide on INCO HPM Ni oxidized at 1300° C. Sample F-26, unetched, 500X.

cracked oxide observed during this investigation. The oxide may have cracked during handling and not during oxidation or cooling to room temperature.

Upon completion of the runs, the oxide layer was green on the INCO HPM nickel for the 1200° C. runs. The oxide was black on the Foundry nickel and National Lead nickel for the 1200° C. runs and also on the INCO HPM nickel for the 1300° C. runs. Extra samples of Foundry nickel and National Lead nickel were oxidized in oxygen for 45 minutes at 1200° C. The oxide on the National Lead nickel was then green while the oxide on the Foundry nickel was still black. A sample of INCO HPM nickel was oxidized for 1.5 minutes at 1200° C. and the oxide was grey. X-ray diffraction patterns for the green and black oxides both agreed with the published data for NiO within 0.05%.

When the oxide layer was removed from any of the samples, a light-green powdery layer of oxide was observed in contact with the nickel. The powdery layer was not analyzed but was assumed to be NiO as reported in the section on Previous Research.[5]

Figure 21 shows the shingle-like structure of the nickel oxide. The oxide crystals are growing predominantly in the (111) plane in the area shown in Figure 21. The growth layers on the oxide crystals are apparent and show the irregularities in thickness even on single crystals.

Figure 22 shows the growth layers on a particular oxide crystal. The large light-colored crystal appears to be growing in the (111) plane. The growth pattern on the large crystal appears similar to a screw dislocation.

Figure 23 shows an area of localized oxide growth on a sample of INCO HPM nickel oxidized for three hours at 1300° C. in a very

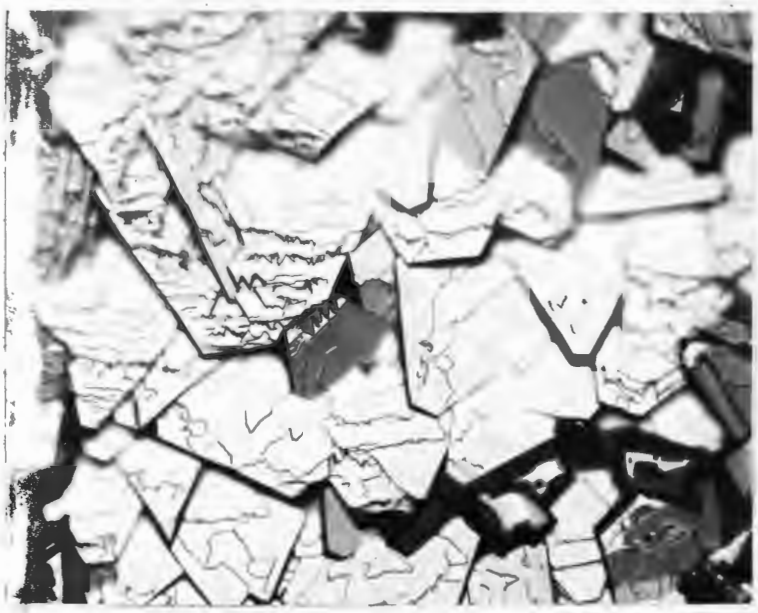

Figure 21. Shingle-like structure of nickel oxide on INCO HPM Ni oxidized at 1300° C. Sample F-23, unetched, 500X.

Figure 22. Nickel oxide on INCO HPM Ni oxidized at 1300° C. Sample F-24, unetched, 250X.

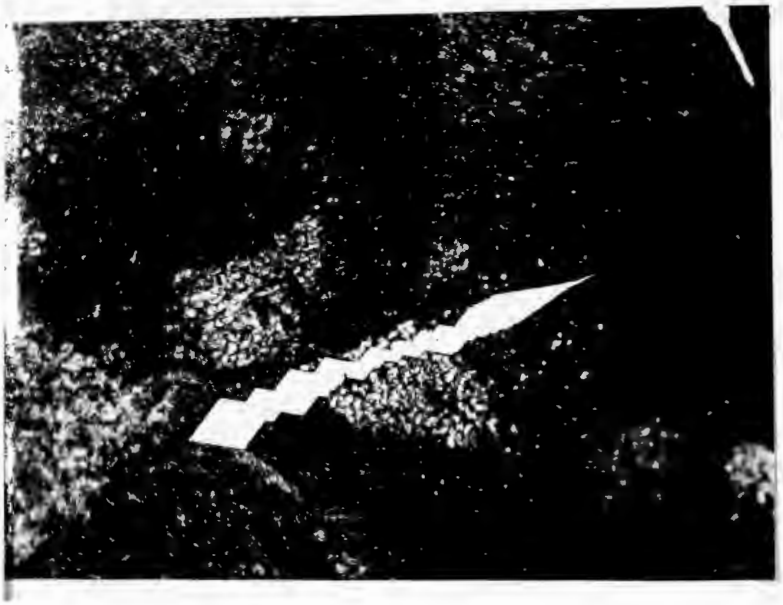

Figure 23. Localized oxide growth and whisker on INCO HPM Ni oxidized at 1300° C. for 3 hours in limited O_2 supply. Unetched, 200X.

limited supply of oxygen. The dark area is only slightly oxidized. The light-colored oxide structure appears to be composed of repeated (110) planes. A whisker, which is believed to be NiO, extends from one end of the oxide structure and curves across it. A large number of such whiskers, which were often in clusters, were observed on this sample.

V. DISCUSSION

Correlation with the Parabolic Rate Law. The agreement of the data with the parabolic rate law is considered to be within the limits of experimental error. The deviation from the parabolic rate law continued for up to 40 minutes. No direct correlation between the end of the period of deviation and the oxide thickness was apparent. Phelps, Gulbransen, and Andrew reported that a deviation from the parabolic rate law may occur during the early stage of oxidation because a monolayer of oxide forms and then lateral growth of crystals starts from scattered nuclei.[17] Figure 23 appears to be an extreme example of such an occurence. The oxide layer must be relatively uniform for the parabolic rate law to apply. Figure 24 shows initial localized oxidation with the dark area oxidized and the light-colored area relatively free of oxidation. It is apparent that the parabolic rate law could not apply for the stage of oxidation shown in Figure 24. The deviation from the parabolic rate law would continue until the surface of the nickel was covered with a uniform oxide layer. Figure 25 shows the relatively even interface between the nickel and the oxide for a period in which the parabolic rate law was applicable. It was difficult to etch the grain boundaries in the high-purity nickel so an etchant was used which preferentially stained certain grains. It appears from Figure 25 that after the oxide layer has reached a certain thickness accelerated attack at the grain boundaries does not occur.

The results of this investigation do not contradict Gulbransen and Andrew who reported a deviation from the parabolic rate law for temperatures over 900° C.[1] The work of Gulbransen and Andrew was

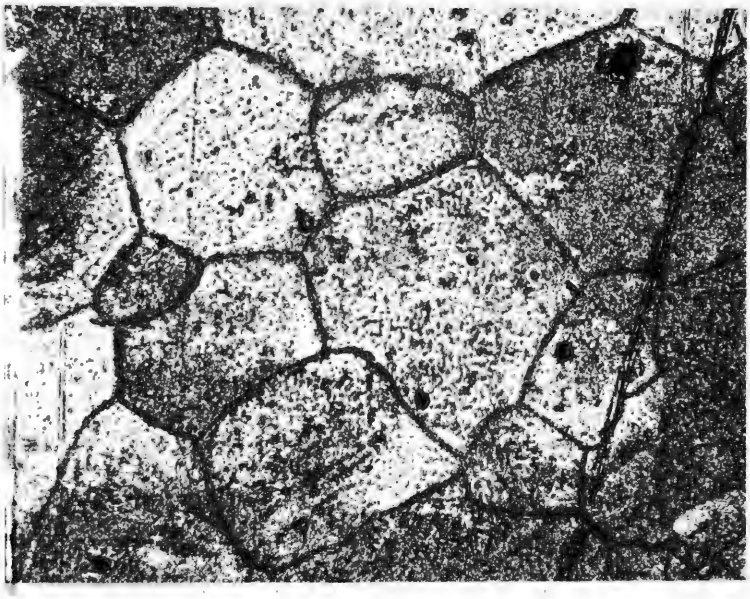

Figure 24. Localized oxidation on INCO HPM Ni oxidized 1.5 min. at 1200° C. Unetched, 250X.

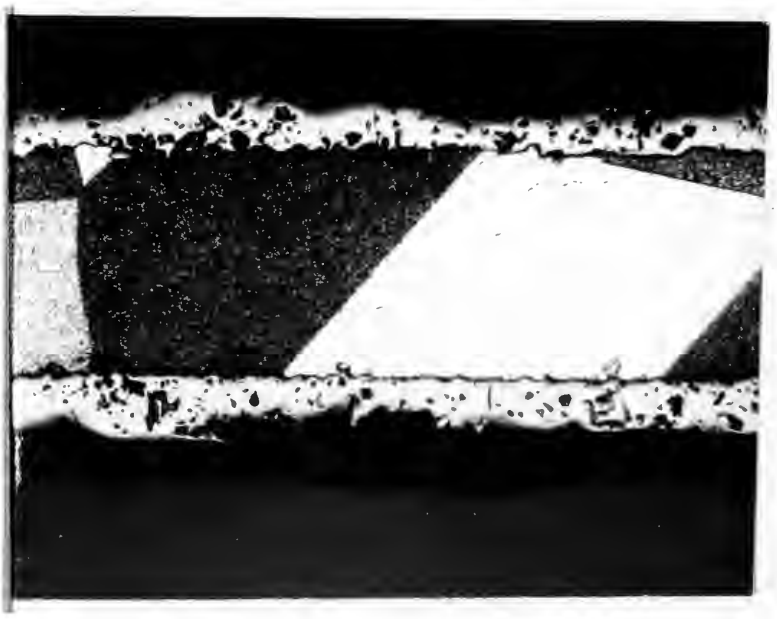

Figure 25. Cross-section of INCO HPM Ni oxidized at 1300° C. Stained with acidified $FeCl_3$, 250X.

limited to temperatures and times which limited the thickness of the oxide layer to the region in which the data for this investigation also departed from the parabolic rate law. Gulbransen and Andrew based part of their conclusions on the change in color of the oxide from gray to green at temperatures over 900° C. Apparently they neglected to consider the possible correlation between thickness and color and concluded that the change in color was due to the oxide layer losing contact with the nickel. The work for this investigation on INCO HPM nickel showed that the oxide is gray when very thin and then green which changes gradually to black as the oxide layer thickens without any noticeable change in the rate of change of the rate of oxidation. X-ray diffraction patterns for the green and black oxides both agreed with the published date for NiO within 0.05%.

Effect of Temperature and Purity. As shown in Figure 10, the effect of temperature on the rate of oxidation of nickel is quite pronounced. At the end of 180 minutes, the oxide layer on INCO HPM nickel at 1300° C. was over twice the thickness of the oxide layer formed at 1200° C.

Due to the number of impurities and the limited nature of this investigation, it was impossible to find a correlation between the change in rate of oxidation or degree of internal oxidation with the change in specific impurities. Figure 10 shows a lower rate of oxidation at 1200° C. with higher purities. According to Kubaschewski and Hopkins, lithium would be the only impurity which would theoretically reduce the rate of oxidation of nickel.[31] Figure 11 and Figure 12 suggest that impurities of the amount present in National Lead nickel and Foundry nickel increase the amount of internal oxi-

dation since no visible internal oxidation was observed with INCO HPM nickel. Figure 12 also suggests that the oxygen may diffuse inward more rapidly along the grain boundaries than through the center of the grains.

The agreement between the amount of impurities and etch pits was as expected since etch pits occur at dislocations which may be caused by impurities. The various geometrically shaped etch pits indicate the orientation of the oxide crystals. Figure 14 shows small etch pits on the (001) plane which are apparently lined up on slip planes in the oxide crystal. Etch pits normally have the geometrical shape of the plane on which they occur but there are no planes in the cubic structure of nickel oxide similar to the etch pits in Figure 15. The unusual etch pits may be on vicinal planes or vicinal hillocks or other deviations from the perfect crystal structure.[32]

Activation Energy. The value of 68,300 cal/mole for the activation energy of oxidation of nickel, which was reported by Gulbransen and Andrew for over 900° C., is believed to be high since the conditions of the investigation were such that the rate of oxidation had not started to follow the parabolic rate law before completion of the runs.[1] The calculated activation energy of 40,700 cal/mole is in close agreement with the activation energy of 41,200 cal/mole reported by Gulbransen and Andrew for below 900° C. where they found the parabolic rate law applicable.[1] The agreement with 44,200 cal/mole reported by Shim and Moore for the activation energy for the diffusion of nickel in nickel oxide (in the range 1000° - 1400° C.) indicates that the value obtained in this investigation is reasonable.[30] The rate of diffusion of nickel in the oxide layer is believed to be the

controlling factor on the rate of oxidation.[8,18,26,30]

Reproducibility of Results. The volumetric oxidation apparatus was found to give reproducible results at 1200° C. with fair agreement between runs at 1300° C. The measured weight change usually agreed with the weight change calculated from the measured volume of oxygen consumed within the degree of accuracy of weighing for the runs at 1200° C. At 1300° C. the measured weight gain was 4-6% lower than the weight gain calculated from the measured volume of oxygen consumed. The vapor pressure of nickel is 4.33×10^{-8} atm at 1193° C. and 9.92×10^{-8} atm at 1234° C.[28] The vapor pressure of NiO is 2.90×10^{-9} atm at 1168° C. and 2.66×10^{-8} atm at 1238° C.[28] The presence of nickel on the wall of the cold portion of the mullite reaction tube indicates that the sublimation may have been of measurable amounts. When substantial amounts of sublimation occur, volumetric or manometric oxidation apparatuses may be found to function more accurately than the gravimetric apparatus normally used to measure the rate of oxidation. The sublimed nickel oxide would have a negligible effect on measurements since it would condense rapidly in the cold end of the mullite reaction tube. It was assumed that the sublimed nickel would oxidize completely during the two minute period in which the rate of reaction could not be measured and would therefore have a negligible effect on the measured amount of oxygen consumed by the reaction on the sample.

The reproducibility of the results with air indicates that the effect of impurities was negligible and that the magnetic stirrer operated satisfactorily to overcome the effect of thermal diffusion.

Oxide Properties and Structure. The absence of cracks in the oxide after oxidation at 1200° C. and 1300° C. and being air quenched to

room temperature shows that a nickel oxide layer must have at least a small degree of ductility. The one cracked oxide shown in Figure 20 may have cracked during handling. The crack was transgranular and appeared to progress across grains in a step-like manner.

The effect of the light-green powdery oxide layer on the mechanism of oxidation of nickel may be very important. Due to the physical difference of the layers, the mechanism or rate of diffusion of nickel through the powdery oxide layer may be distinctly different from that in the outer oxide layer. It is possible that the inner oxide layer controls the rate of oxidation of nickel after the initial period of deviation from the parabolic rate law.

The irregularities in thickness of single oxide crystals and the shingle-like structure of nickel oxide shown in Figure 21 shows that the oxide layer is not of constant thickness. This may cause a small amount of deviation from the parabolic rate law even after the initial period of deviation.

The whisker shown in Figure 23 is believed to be NiO. Gulbransen and Copan have reported the growth of oxide whiskers during oxidation of various metals.[33] They proposed that surface diffusion may be the method of growth of the whiskers. The whiskers may grow by a screw dislocation process similar to the crystals as is suggested by Figure 22. Many of the whiskers observed in this investigation were in the range of 0.02 - 0.04 cm long.

VI. CONCLUSIONS

Conclusions. The rate of oxidation of nickel of the three purities oxidized at 1200° C. and of the INCO HPM nickel oxidized at 1300° C. follows the parabolic rate law for a minimum of 140 minutes after an initial period of deviation which lasted up to 40 minutes. During the initial period of deviation, the rate of oxidation does not decrease rapidly enough for the parabolic rate law to be applicable.

The agreement with the parabolic rate law is shown by Figure 8, Figure 9, and Table II. Figure 8 is a parabolic plot of the averaged data for each set of conditions investigated. The agreement of the data with straight lines shows the agreement with the parabolic rate law. Figure 9 is a log-log plot for the averaged data for each set of conditions investigated. The initial period of deviation is shown by the sections of the curves which fail to fall on the straight lines. The applicability of the parabolic rate law is also shown by the agreement of the curves in Figure 9 with straight lines whose slope is approximately the 0.50 for the parabolic equation. The slope of the straight-line portions of the curves in Figure 9 were calculated by the method of least squares and are shown in Table II.

Figure 23 and Figure 24 show causes for the initial deviation from the parabolic rate law. Figure 23 shows that after an initial oxide layer forms, localized nucleation occurs with concentrated growth at specific points. Figure 24 shows that accelerated attack occurs at the grain boundaries and in localized areas on the nickel grains.

A uniform layer is necessary for the parabolic rate law to be applicable. Figure 21 shows that the oxide layer is of varying thickness even after 180 minutes of oxidation with a shingle-like structure

and also with various layers within each oxide crystal.

The rate of oxidation is very sensitive to temperature and purity. Figure 10 shows the effect of 100° C. difference on the rate of oxidation of INCO HPM nickel at 1200° C. and 1300° C. After 180 minutes, the samples at 1300° C. had oxidized twice as much as those at 1200° C. Figure 10 also shows the effect of purity on the rate of oxidation at 1200° C. The combinations of impurities present in the Foundry nickel and National Lead nickel decreased the resistance of nickel to oxidation.

The volumetric apparatus developed for this investigation provides a satisfactory method for measuring the rate of reaction for processes involving the consumption of a gaseous reactant. The temperature limitation of the apparatus would be the temperature at which the mullite reaction tube failed to remain impervious to gases.

Suggestions For Future Research. There are several phases of this investigation and related phenomena that are worthy of further investigation. Some of the following suggestions would require very special equipment but the results would add greatly to our understanding of the mechanism of oxidation of metals and the effect of impurities.

(1) Precision X-ray work should be carried out on the green and black nickel oxide to definitely establish the basis for the difference in color.

(2) The effect of controlled amounts of specific impurities and combinations of impurities on the rate of oxidation of nickel should be investigated. Emphasis should be placed on lithium which was reported to be the only impurity which would theoretically reduce the rate of oxidation of nickel.[31]

(3) An investigation should be carried out to determine whether the impurities in the metal tend to concentrate at the oxide-metal interface or whether they are evenly distributed in the oxide layer or layers.

(4) The ductility of oxides at elevated temperatures should be investigated. The ductility of the oxide determines partly the ability of the oxide to remain adherent to the residing metal surface. One method would be to oxidize completely relatively large nickel samples to determine whether a vacancy would exist or whether the oxide layer could continue to remain adherent to the residing metal surface until completion. A similar investigation was carried out on iron by Juenker, Meussner, and Birchenall.[34]

(5) The rate of oxidation of nickel and similar metals should be measured at elevated temperatures approaching the melting point.

VII. APPENDIX

Table V

Test: F-11

National Lead Nickel
Area - 2.464 cm^2

Temperature - 1200° C.
Atmosphere - Oxygen
Pressure - 0.555 atm.

Measured weight gain - 12.0 mg
Calculated weight gain - 11.8 mg

time (min.)	volume (cm^3)	wt. gain (mg/cm^2)	time (min.)	volume (cm^3)	wt. gain (mg/cm^2)
3.3	1.304	0.374	45	7.668	2.198
5	1.938	0.555	50	8.028	2.301
6.7	2.385	0.684	55	8.419	2.413
8.3	2.793	0.800	60	8.786	2.518
10	3.252	0.932	67.7	9.194	2.635
11.7	3.608	1.034	73.3	9.651	2.766
13.3	3.925	1.125	83.3	10.267	2.943
15	4.242	1.216	91.7	10.742	3.079
16.7	4.523	1.296	100	11.208	3.212
18.3	4.772	1.368	105	11.461	3.285
20	4.954	1.420	108.3	11.636	3.335
21.7	5.184	1.486	116.7	11.967	3.430
23.3	5.395	1.546	126.7	12.464	3.572
25	5.597	1.604	140	12.910	3.700
26.7	5.793	1.660	160	13.727	3.934
31.7	6.343	1.818	176.7	14.519	4.161
33.3	6.501	1.863	183.3	14.772	4.233
35	6.630	1.900	200	15.349	4.399
38.3	6.948	1.991	233.3	16.515	4.733
41.7	7.305	2.094	238.3	16.690	4.783

Table VI

Test: F-12

National Lead Nickel
Area - 2.460 cm^2

Temperature - 1200° C.
Atmosphere - Oxygen
Pressure - 0.688 atm.

Measured weight gain - 14.0 mg
Calculated weight gain - 14.2 mg

time (min.)	volume (cm^3)	wt. gain (mg/cm^2)	time (min.)	volume (cm^3)	wt. gain (mg/cm^2)
3.3	1.429	0.508	31.7	5.930	2.107
5	1.938	0.689	33.3	6.065	2.155
6.7	2.368	0.841	36.7	6.304	2.240
8.3	2.787	0.990	40	6.632	2.356
10	3.128	1.111	46.7	7.129	2.533
11.7	3.429	1.218	56.7	7.838	2.785
13.3	3.726	1.324	66.7	8.582	3.049
15	3.984	1.416	83.3	9.555	3.395
16.7	4.236	1.505	100	10.514	3.736
18.3	4.446	1.580	116.7	11.309	4.018
20	4.684	1.664	120	11.459	4.071
21.7	4.886	1.736	137.5	12.097	4.298
23.3	5.072	1.802	157.5	12.925	4.592
25	5.250	1.865	181.7	13.796	4.902
26.7	5.424	1.927	245.5	15.911	5.653
28.3	5.602	1.990	256	16.215	5.761
30	5.786	2.056	261.7	16.285	5.786

Table VII

Test: F-13

National Lead Nickel
Area - 3.068 cm^2

Temperature - 1200° C.
Atmosphere - Oxygen
Pressure - 0.684 atm.

Measured weight gain - 10.0 mg
Calculated weight gain - 9.9 mg

time (min.)	volume (cm^3)	wt. gain (mg/cm^2)	time (min.)	volume (cm^3)	wt. gain (mg/cm^2)
3.3	1.193	0.338	26.3	5.474	1.550
5	1.726	0.489	30.8	5.884	1.666
6.7	2.168	0.614	33.3	6.125	1.735
8.3	2.567	0.727	36.7	6.472	1.833
10	2.925	0.828	41.7	6.914	1.958
11.7	3.262	0.924	50	7.623	2.159
13.3	3.560	1.008	58.3	8.257	2.338
15	3.881	1.099	68.3	9.016	2.553
16.7	4.146	1.174	83.3	10.078	2.854
20	4.654	1.318	100	11.081	3.138
23.3	5.092	1.442	105	11.381	3.223

Table VIII

Test: F-14

Foundry Nickel
Area - 2.569 cm^2

Temperature - 1200° C.
Atmosphere - Air
Pressure - 0.803 atm.

Measured weight gain - 11.9 mg
Calculated weight gain - 11.6 mg

time (min.)	volume (cm^3)	wt. gain (mg/cm^2)	time (min.)	volume (cm^3)	wt. gain (mg/cm^2)
4.2	1.306	0.518	33.3	5.375	2.134
5	1.525	0.605	36.7	5.727	2.274
6.7	1.834	0.728	38.3	5.887	2.337
8.3	2.008	0.797	41.7	6.232	2.474
10	2.235	0.887	50	6.741	2.676
11.7	2.700	1.072	58.3	7.181	2.851
13.3	3.021	1.199	66.7	7.712	3.062
15	3.229	1.282	75	8.158	3.239
16.7	3.606	1.432	83.3	8.592	3.411
20	4.015	1.594	100	9.452	3.752
23.3	4.451	1.767	116.7	10.279	4.081
26.7	4.850	1.925	133.3	11.109	4.410
30	5.096	2.023	139	11.384	4.519

Table IX

Test: F-15

Foundry Nickel
Area - 2.500 cm^2

Temperature - 1200° C.
Atmosphere - Air
Pressure - 0.846 atm.

Measured weight gain - 13.8 mg
Calculated weight gain - 14.3 mg

time (min.)	volume (cm^3)	wt. gain (mg/cm^2)	time (min.)	volume (cm^3)	wt. gain (mg/cm^2)
3.3	0.915	0.393	39	6.027	2.591
5	1.481	0.637	41.7	6.227	2.677
6.7	1.917	0.824	50	6.869	2.953
8.3	2.213	0.951	58.3	7.392	3.178
10	2.531	1.088	66.7	8.010	3.443
11.7	2.864	1.231	75	8.485	3.648
13.3	3.074	1.322	88.3	9.127	3.924
15	3.370	1.449	116.7	10.258	4.410
16.7	3.631	1.561	133.3	10.871	4.673
20	4.048	1.740	150	11.407	4.904
23.3	4.436	1.907	153	11.487	4.938
26.7	4.836	2.079	167	11.891	5.112
30	5.188	2.230	192	12.564	5.401
33.3	5.489	2.360	217	13.190	5.670
37.3	5.837	2.509	223	13.340	5.735

Table X

Test: F-16

Foundry Nickel
Area - 2.385 cm^2

Temperature - 1200° C.
Atmosphere - Air
Pressure - 0.875 atm.

Measured weight gain - 12.6 mg
Calculated weight gain - 12.7 mg

time (min.)	volume (cm^3)	wt. gain (mg/cm^2)	time (min.)	volume (cm^3)	wt. gain (mg/cm^2)
1.7	0.500	0.233	75	7.076	3.297
3.3	0.966	0.450	91.7	7.749	3.610
5	1.327	0.618	98.3	8.153	3.798
6.7	1.679	0.782	108.3	8.612	4.012
8.3	2.053	1.173	120.7	8.943	4.167
11.7	2.517	1.173	133.3	9.280	4.324
16.7	3.143	1.464	145	9.567	4.457
25	3.935	1.833	155	9.848	4.588
33.3	4.818	2.245	175	10.510	4.897
41.7	5.367	2.500	192	10.969	5.110
50	5.826	2.714	200	11.132	5.186
53.3	6.011	2.801	208	11.343	5.285
63.3	6.561	3.057	214	11.443	5.331

Table XI

Test: F-24

INCO HPM Nickel
Area - 1.685 cm^2

Temperature - 1300° C.
Atmosphere - Oxygen
Pressure - 0.888 atm.

Measured weight gain - 9.2 mg
Calculated weight gain - 9.6 mg

time (min.)	volume (cm^3)	wt. gain (mg/cm^2)	time (min.)	volume (cm^3)	wt. gain (mg/cm^2)
2	0.420	0.281	34	3.612	2.418
3	0.629	0.421	37	3.719	2.489
4	0.719	0.481	44	4.065	2.721
5	0.897	0.600	51	4.375	2.929
6	1.075	0.720	57	4.543	3.041
8	1.316	0.881	67	4.979	3.333
10	1.568	1.050	77	5.327	3.566
12	1.811	1.212	86	5.607	3.753
14	2.029	1.358	91	5.747	3.847
16	2.286	1.530	107	6.230	4.170
19	2.519	1.686	127	6.869	4.598
22	2.758	1.846	145	7.350	4.920
25	3.001	2.009	157	7.717	5.166
28	3.269	2.188	167	8.211	5.496
31	3.485	2.333	186	8.493	5.685

Table XII

Test: F-26

INCO HPM Nickel
Area - 2.932 cm^2

Temperature - 1300° C.
Atmosphere - Oxygen
Pressure - 0.792 atm.

Measured weight gain - 23.1 mg
Calculated weight gain - 24.1 mg

time (min.)	volume (cm^3)	wt. gain (mg/cm^2)	time (min.)	volume (cm^3)	wt. gain (mg/cm^2)
2	1.350	0.463	52	12.038	4.130
3	2.045	0.702	55	12.342	4.235
4	2.576	0.884	63	13.216	4.534
5	3.083	1.058	69	13.852	4.753
6	3.511	1.205	75	14.388	4.937
7	3.914	1.343	79	14.809	5.081
9	4.622	1.586	86	15.386	5.279
12	5.483	1.881	90	15.764	5.409
15	6.316	2.167	97.6	16.359	5.613
18	6.932	2.378	106.7	17.051	5.850
20	7.361	2.526	113	17.493	6.002
22	7.781	2.670	123	18.132	6.221
24	8.148	2.796	133	18.869	6.474
26	8.487	2.912	140	19.313	6.626
28	8.789	3.016	148	19.841	6.807
30	9.109	3.125	159	20.520	7.040
33	9.564	3.281	169	21.079	7.232
36	9.977	3.423	178.3	21.728	7.455
39	10.411	3.572	189	22.161	7.603
43	10.943	3.755	196	22.534	7.731
46	11.328	3.887	213	23.353	8.012
49	11.691	4.011	224	23.909	8.203

Table XIII

Test: F-27

INCO HPM Nickel
Area - 2.546 cm^2

Temperature - 1300° C.
Atmosphere - Oxygen
Pressure - 0.818 atm.

Measured weight gain - 16.6 mg.
Calculated weight gain - 17.6 mg.

time (min.)	volume (cm^3)	wt. gain (mg/cm^2)
2.6	1.424	0.581
4	2.017	0.823
5	2.382	0.972
6	2.749	1.122
7	3.045	1.243
8.5	3.452	1.409
10	3.867	1.578
12	4.290	1.751
14	4.670	1.906
16	5.046	2.059
18	5.376	2.194
20	5.703	2.327
22	5.970	2.436
25	6.345	2.589
28	6.711	2.739
30	6.962	2.841
33	7.317	2.986
36	7.657	3.125
39	7.992	3.262
43	8.434	3.442
47	8.861	3.616
50	9.178	3.746
55	9.672	3.947
60	10.131	4.134
65	10.491	4.281
72	10.683	4.360
80	11.180	4.563
84	11.459	4.676
86	11.599	4.734
96	12.193	4.976
105	12.789	5.219
114	13.339	5.444
125	14.015	5.720
135	14.622	5.967
145	15.169	6.190
155	15.715	6.413
170	16.494	6.731
178	16.966	6.924

Table XIV

Test: F-28

INCO HPM Nickel
Area - 3.926 cm^2

Temperature - 1200° C.
Atmosphere - Oxygen
Pressure - 0.708 atm.

Measured weight gain - 13.9 mg
Calculated weight gain - 13.8 mg

time (min.)	volume (cm^3)	wt. gain (mg/cm^2)
2.6	1.278	0.293
3.5	1.626	0.373
4.5	1.974	0.452
6	2.348	0.538
8	2.851	0.653
10	3.241	0.743
12	3.502	0.802
14	3.764	0.862
16	4.069	0.932
19	4.490	1.029
22	4.894	1.121
25	5.270	1.207
28	5.599	1.283
33	6.100	1.398
37	6.559	1.503
39	6.795	1.557
42	7.081	1.622
45	7.337	1.681
48	7.678	1.759
51	7.913	1.813
55	8.204	1.880
61	8.709	1.995
67	9.084	2.081
72	9.456	2.166
77	9.774	2.239
82	10.198	2.336
87	10.520	2.410
94	10.859	2.488
100	11.188	2.563
108	11.611	2.661
116	11.976	2.744
124	12.361	2.832
132	12.842	2.942
138	13.048	2.989
148	13.521	3.098
155	13.802	3.162
165	14.261	3.267
175	14.596	3.344
185	14.981	3.432
195	15.380	3.524

Test: F-29

INCO HPM Nickel
Area - 4.021 cm^2

Temperature - 1200° C.
Atmosphere - Oxygen
Pressure - 0.753 atm.

Measured weight gain - 14.4 mg
Calculated weight gain - 14.2 mg

time (min.)	volume (cm^3)	wt. gain (mg/cm^2)
2.8	1.120	0.266
4.2	1.541	0.367
5.6	1.879	0.447
7	2.189	0.521
9	2.639	0.628
11	3.047	0.725
13	3.353	0.798
15	3.629	0.863
18	4.027	0.958
21	4.437	1.056
24	4.811	1.146
27	5.156	1.227
30	5.457	1.298
33	5.761	1.371
38	6.180	1.470
41	6.508	1.548
44	6.872	1.635
49	7.208	1.715
53	7.476	1.779
58	7.954	1.892
62	8.226	1.957
66	8.461	2.013
70	8.662	2.061
76	9.056	2.154
81	9.399	2.236
86	9.648	2.295
90	9.760	2.322
95	9.971	2.372
100	10.239	2.436
107	10.587	2.519
112	10.819	2.574
117	11.015	2.620
120	11.173	2.658
126	11.404	2.713
129	11.520	2.741
137	11.886	2.828
152	12.545	2.984
164	13.081	3.112
172	13.423	3.193
187	14.019	3.335
195	14.296	3.401
206	14.828	3.528

Table XVI

Test: F-30

INCO HPM Nickel
Area - 4.079 cm^2

Temperature - 1200° C.
Atmosphere - Oxygen
Pressure - 0.741 atm.

Measured weight gain - unknown*
Calculated weight gain - 13.1 mg

time (min.)	volume (cm^3)	wt. gain (mg/cm^2)	time (min.)	volume (cm^3)	wt. gain (mg/cm^2)
2	0.430	0.099	56	7.364	1.700
3	0.824	0.190	59	7.616	1.758
4	1.139	0.263	62	7.819	1.805
6	1.734	0.400	65	8.050	1.858
7	2.006	0.463	69	8.303	1.916
8	2.191	0.506	76	8.685	2.004
9	2.407	0.556	82	9.129	2.107
10	2.583	0.596	88	9.508	2.194
13	3.123	0.721	97	9.996	2.307
17	3.796	0.876	104	10.409	2.402
20	4.192	0.968	109	10.612	2.449
23	4.571	1.055	115	10.899	2.515
26	4.885	1.127	120	11.099	2.562
29	5.180	1.196	127	11.385	2.628
33	5.551	1.281	133	11.733	2.708
37	5.868	1.354	140	12.119	2.797
39	6.003	1.385	151	12.584	2.904
41	6.146	1.418	160	13.051	3.012
49	6.841	1.579	171	13.522	3.121
52	7.071	1.632	180	13.932	3.216

*Run continued for a total of 22 hours to check the effect of thickness on color. The oxide was black at 8.56 mg/cm^2.

VIII. BIBLIOGRAPHY

12. CAMPBELL, W. E. and U. B. Thomas (1947) The oxidation of metals. Electrochem. Soc. J. 91, p. 623-639.

2. DOERR, R. M. (1959) Personal communication.

18. DRAVNIEKS, A. (1953) Correlation between parabolic oxidation of metals and properties of oxides. Electrochem. Soc. J. 100, p. 95-102.

19. FINCH, G. I. and K. P. SINHA, (1957) A new superstructure of nickel oxide. Faraday Soc. Trans. 53, p. 623-627.

22. FOLEY, R. T. and C. J. GUARE, (1959) The oxidation of iron-nickel alloys. Electrochem. Soc. J. 106, p. 936-940.

4. FREDERICK, S. F. and I. CORNET (1955) The effect of cobalt on the high temperature oxidation of nickel. Electrochem. Soc. J. 102, p. 285-291.

25. GULBRANSEN, E. A. (1949) Kinetics and structural factors involved in the oxidation of metals. Ind. Eng. Chem. 41, p. 1385 - 1391.

21. GULBRANSEN, E. A. (1947) The kinetics of oxide film formation on metals and alloys. Electrochem. Soc. Trans. 91, p. 573-604.

11. GULBRANSEN, E. A. (1944) A vacuum microbalance for the study of chemical reactions on metals. Rev. Sci. Instr. 15, p. 201-204.

1. GULBRANSEN, E. A. and K. F. ANDREW (1947) High temperature oxidation of high purity nickel between 750° and 1050° C. Electrochem. Soc. J. 104, p. 451-454.

8. GULBRANSEN, E. A. and K. F. ANDREW (1954) The kinetics of oxidation of high purity nickel. Electrochem. Soc. J. 101, p. 128-140.

33. GULBRANSEN, E. A. and T. P. COPAN (1959) Effect of stress on unusual crystal habits of corrosion products on iron, nickel, chromium, and stainless steel. In: Internal stresses and fatigue in metals (a symposium). Amsterdam, Elsevier, p. 397-410.

9. GULBRANSEN, E. A. and J. W. HICKMAN (Oct. 1946) An electron diffraction study of oxide films formed on iron, cobalt, nickel, chromium, and copper at high temperatures. Metals Technology 13, p. 1-26.

23. HAHN, H. and A. KONRAD (1951) Uber die bildungswarme des Ni_3N (On the heat of formation of Ni_3N.) Z. anorg. allg. Chem. 264, p. 181-183.

32. HONESS, A. P. (1927) The nature, origin and interpretation of the etch figures on crystals. New York, Wiley, p. 34-43.

27. INCO TECHNICAL BULLETIN (Sept. 1959) Annealing nickel, monel, and inconel. T-20, p. 6-7.

3. JENKINS, A. E. (1955-1956) A further study of the oxidation of Ti and its alloys at elevated temperatures. Inst. Met. J. 84, p. 1-9.

28. JOHNSTON, H. L. and A. L. MARSHALL (1940) Vapor pressures of nickel and of nickel oxide. Am. Chem. Soc. J. 62, p. 1382-1390.

34. JUENKER, D. W., R. A. MEUSSNER, and C. E. BIRCHENALL (Jan. 1958) Cavity formation in iron oxide. Corrosion 14, p. 57-64.

10. KUBASCHEWSKI, O. and B. E. HOPKINS (1953) Oxidation of metals and alloys. London, Buttersworth, p. 68-69.

16. KUBASCHEWSKI, O. and B. E. HOPKINS (1953) Oxidation of metals and alloys. London, Buttersworth, p. 43.

20. KUBASCHEWSKI, O. and B. E. HOPKINS (1953) Oxidation of metals and alloys. London, Buttersworth, p. 71.

29. KUBASCHEWSKI, O. and B. E. HOPKINS (1953) Oxidation of metals and alloys. London, Buttersworth, p. 49.

31. KUBASCHEWSKI, O. and B. E. HOPKINS (1953) Oxidation of metals and alloys. London, Buttersworth, p. 145.

24. LYMAN, T. (ed.) (1948) The metals handbook. Cleveland, American Society for Metals, p. 1231.

26. MOORE, W. J. and J. K. LEE (1952) Kinetics of the formation of oxide films on nickel foil. Faraday Soc. Trans. 48, 916-920.

7. MOORE, W. J. and J. K. LEE (1951) Oxidation kinetics of nickel and cobalt. J. Chem. Physics 19, p. 255.

17. PHELPS, R. T., E. A. GULBRANSEN and J. W. HICKMAN (1946) Electron diffraction and electron microscope study of oxide films formed on metals and alloys at moderate temperatures. Ind. Eng. Chem. (Anal.) 18, p. 391.

14. PILLING, N. B. and R. E. BEDWORTH (1923) The oxidation of metals at high temperatures. Inst. Met. J. 29, p. 529-582.

5. PREECE, A. and G. LUCAS (1952) The high-temperature oxidation of some cobalt-base and nickel-base alloys. Inst. Met. J. 81, p. 219-227.

30. SHIM, M. T. and W. J. MOORE (1957) Diffusion of nickel in nickel oxide. J. Chem. Physics 26, p. 802-804.

15. TAMMANN, G. (1920) Uber anlauffarben von metallen (On temper colors of metals.) Z. anorg. Chem. 111, p. 78-89.

13. TRONSTAD, L. (1933) The investigation of thin surface films on metals by means of polarized light. Faraday Soc. Trans. 29, p. 502-504.

6. UHLIG, H., J. PICKETT, and J. MACNAIRN (1959) Initial oxidation rate of nickel and effect of the Curie temperature. Acta Metallurgica 7, p. 111.

VITA

Virgil R. Friebel was born January 17, 1932, in Britton, South Dakota. He received his elementary education and secondary schooling in the public school system in South Dakota.

He attended Northern State Teachers College from September 1950, to June 1952.

In September 1952 he entered the military service where he spent four years. At the time of his release from the military service he was a Naval Aviator and a 1st Lieutenant in the U. S. Marine Corps.

He returned to college in September 1956, and received the degree Bachelor of Science in Metallurgical Engineering from South Dakota School of Mines and Technology in June 1959.

In September 1959, he entered the School of Mines and Metallurgy of the University of Missouri for graduate work in Metallurgy.

He is married and the Friebels have two children.